5-2017

The “Apparent” Diffusion Coefficient of Electrons Through a Nafion Membrane

Marissa Kayle Reynolds
University of Arkansas, Fayetteville

The "Apparent" Diffusion Coefficient of Electrons Through a Nafion Membrane

A thesis submitted in partial fulfillment
of the requirements for the degree of
Master of Science in Chemistry

by

Marissa Kayle Reynolds
Arkansas Tech University
Bachelor of Science in Chemistry, 2013

May 2017
University of Arkansas

This thesis is approved for recommendation to the Graduate Council.

_____
Dr. David W. Paul
Thesis Director

_____
Dr. Ingrid Fritsch
Committee Member

_____
Dr. Bill Durham
Committee Member

Abstract

The hydrogen/oxygen fuel cell is a greener, more efficient energy solution. However, there are many problems with the fuel cell including storage, infrastructure, cost, the oxygen reduction reaction, and the durability of the proton exchange membrane (PEM). The PEM is not only used as the electrolyte for the cell but also as a physical barrier between the anode and the cathode. The integrity of this membrane is crucial to the functioning of the fuel cell. This thesis will examine using ferricyanide as a probe molecule for diagnostic experiment of Nafion membrane integrity. Using hydrodynamic voltammetry with a rotating disk electrode (RDE), the signals between a bare electrode surface and one modified with a Nafion membrane can be differentiated to observe if there are any discrepancies in the membrane coverage of the electrode.

During this work, ferricyanide was observed to incorporate into the membrane during a hydration period in the solution. Different mechanisms of how this incorporated concentration affects the current response are discussed, concluding electron-hopping is the most plausible mechanism for the case at hand. The Tedford Equation was formulated model the hydrodynamic current response in the membrane taking into account rotation rate dependence and the apparent diffusion of electrons through the membrane.

Acknowledgements

First and foremost, I thank my Lord, my God who in all His awesome wonder put me on this path and brought me to where I am today. Without Him, none of this would be possible, nor would it hold any meaning. It has been a true blessing to study the field of chemistry and observe first-hand how beautifully His hand formed the most basic and original parts of this universe and how each part works together and compliments each other.

Second, I must thank Dr. David Paul (DP) for his constant encouragement not only as an advisor and mentor, but also as a friend. His insight and wisdom has helped me learn and understand more in this work than I knew was possible. His and Mrs. DP's kindness and generosity are unconditional and beyond deserving.

I would like to thank my committee members, Dr. Ingrid Fritsch and Dr. Bill Durham, for taking their valuable time to teach, encourage, and mold the minds of upcoming chemists. Thank you for continuing to impart your knowledge to the new generations.

I am overwhelmingly thankful to my husband, Chris. Without his love and support, this work would not be possible. Thank you for motivating me when I needed it and for everything that you do to make our lives extraordinary. I love you most.

Thank you to my mom and dad for your unwavering love and support in my whole life. Thank you for listening when I ramble and for filling my life with adventure. Love you forever, like you for always.

Thank you to my EH&S family for your constant support, votes of confidence, and bottomless cups of coffee. You have all helped me prepare for my future with all the talks, trainings, and tacos and for that I am forever grateful.

Thank you to those music makers that have kept me company in my long stints of readings, writings, and productivity. Specifically, to Tom Petty and the Heartbreakers for being the soundtrack in my attempt to run down this dream and to Train who I can always count on to be my parachute.

Thank you to my Brothers in Alpha Chi Sigma and to all other family, friends, and those I am honored to call both. Thank you for creating such an extensive and enduring support system for me. It was a crucial contribution to this achievement.

Finally, this thesis is completed in honor of my Uncle Ted. Thank you for all your advice and your help in my math homework. My name would not be on the sidewalk without your help.

Hit it.

Table of Contents

Table of Figures

Table of Equations

1 INTRODUCTION

1.1 BRIEF HISTORY OF THE FUEL CELL

In the mid-1880's, Karl Friedrich Benz (Germany) invented the first gasoline fueled automobile.[8] The vehicle was powered by an internal combustion engine that was the first of countless to come. By the 1970's there were over 100 million registered vehicles in the United States, and by 2012 there were over 250 million.[9] The combustion engine was widely accepted because they are more efficient and/or convenient than their steam or electric counterparts available at the time.[10]

As technology improved, society began looking for a replacement for the combustion engine. This replacement needed to be cheaper, more efficient, and most of all more environmentally friendly. The obvious choice was an electric motor with a mobile source of electricity such as fuel cells or batteries. There are two scientists credited with the invention of the fuel cell.[3] Christian Friederich Schonbein published a paper in 1839[11] where he discussed an electrochemical reaction involving hydrogen and oxygen to create a current. In the following issue[12], Sir William Robert Grove discussed a reaction involving water that produced electricity. Ulf Bossel would later explain in his book, *The Birth of the Fuel Cell*, that Schoebein should be given credit for the fuel cell effect, but Grove credited with the invention of the fuel cell itself.[13]

Today, combustion engines are still the preferred method of energy consumption (especially in transportation). But, the combustion of gasoline creates exhausts that are harmful to the planet's atmosphere and its fuel is a limited resource. Eventually the planet's cache of fossil fuel will be exhausted and a replacement will be necessary. Fuel cells replace the energy from combustion with energy from electrochemical processes. This would solve three of the major problems seen with combustion engines: the finite source of fossil fuel, the environmental

hazards and complications of drilling, and the exhaust from the fuel. Hydrogen/oxygen fuel cells would need hydrogen gas as the fuel and oxygen gas as the oxidant. If these gases are pure, the only exhaust from the fuel cell would be water and heat. While some of this hydrogen will come from natural gas, there are also other sources such as water electrolysis and biomass.

The United States only produces forty percent of the fossil fuel consumed. The rest comes from other areas such as Latin America, Canada, and the Persian Gulf. But, no matter where the oil comes from, when there is a change in price in one area, all other areas of the economy are affected.[14] By using other fuel sources, a great weight would be lifted as the U.S. would no longer need to rely on other countries and their oil exports.

1.2 PROTON EXCHANGE MEMBRANE FUEL CELLS

A proton exchange membrane fuel cell (PEMFC) converts chemical energy into electrical energy for uses in transportation, power sources, and other like items. Fuel cells/electric motors are preferable to combustion engines because they are more efficient; their only exhaust is water and they operate at lower temperatures. However, there are problems to work out before their use will be competitive to that of the fossil fuel driven combustion engine: they are very expensive to construct, the necessary reduction of oxygen is limited by electron transfer kinetics, and there are problems with both chemical and mechanical degradation. This work will touch on the degradation problems by looking at the chemical and mechanical durability of Nafion as a proton exchange membrane (PEM).

The fuel cell works by forcing hydrogen gas (H_2) and oxygen gas (O_2) to undergo an oxidation-reduction reaction in which the products are water and heat.

$$2H_2 + O_2 \rightarrow 2H_2O + \Delta \qquad \textit{Eq. 1.1}$$

The reactants are separated in two half-cells with the energy harvested from electrons flowing through an external circuit. A schematic for a proton exchange membrane fuel cell (PEMFC) is shown in Figure 1. At the anode, hydrogen gas is oxidized to protons and electrons. The protons diffuse through the proton exchange membrane (PEM) arriving at the cathode where the oxygen gas is reduced. The protons, the reduced oxygen, and the electrons from the external circuit combine to form water with an exothermic reaction with a standard enthalpy of -63 kcal/mol.[15] Without considering electron transfer kinetics (a big consideration in the case of oxygen) the E^o for hydrogen/hydrogen ion is at 0.0 V, and for oxygen/water is +1.23 V.[16] Because of this potential difference, there is a very large thermodynamic advantage for the electrons to go through the external circuit to oxygen at the cathode. Ideally the PEM should only allow protons to migrate through it. As it will be discussed later, this is not always true and this point is a major theme in this thesis.

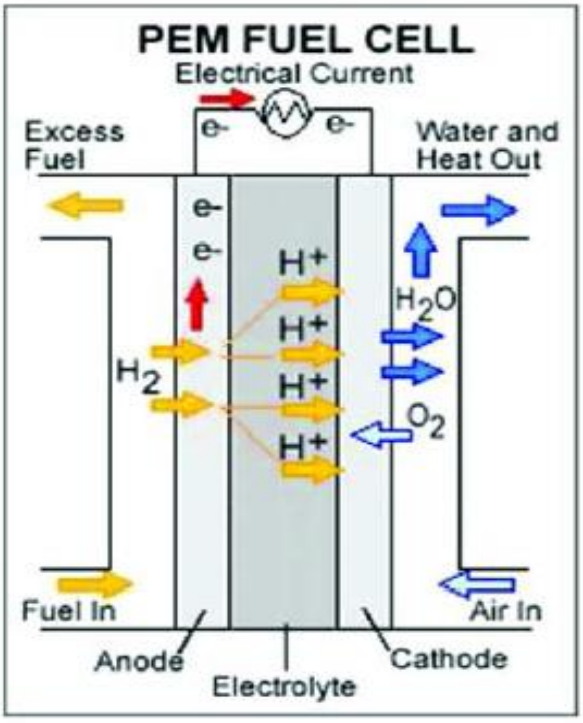

Figure 1. General schematic for a proton exchange membrane fuel cell using hydrogen gas (H2) as the fuel, oxygen gas (O2) as the oxidant, and producing an electrical current as well as the byproducts of water and heat.[3]

1.3 Ferricyanide as a Probe Molecule for Nafion Degradation Diagnostics

Typically, Nafion is the polymer membrane used for the PEM. There are two main structures to a Nafion membrane. Figure 2A shows the fluorocarbon backbone which provides

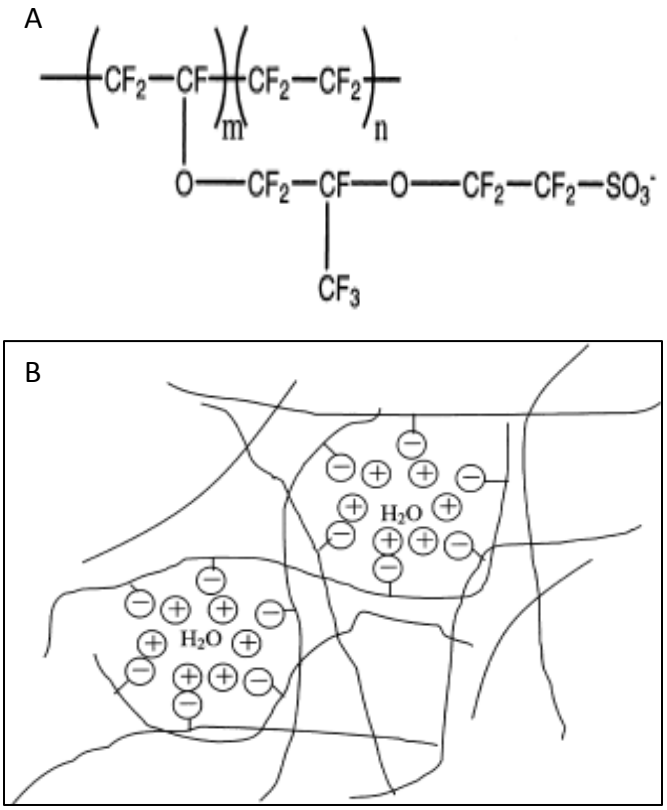

Figure 2. A) Polymer unit of a Nafion membrane and B) the hydrated ion channels at the membrane/solution interface.[4]

the thermal and mechanical strength and the hydrophilic negatively charged sulfonate group determines the ion transport properties. The membrane needs to be hydrated in order to transport protons. The theory is that solution filled ion channels are formed at the hydrophlic membrane/solution interface as shown in Figure 2B. When the membrane swells it puts the polymer backbone under tension. This can cause cracks or tears in the membrane causing the fuel and the oxiant to mix. Currently, thre are no in situ techniques to study Nafion integrity. Outlined in this thesis is the use of ferricyanide as a probe molecule to test membrane integrity. Ferricyanide was chosen because it is well studied, the redox peaks are easily observed, and it is a larger negative ion. This last point is advantageous because Nafion is designed to be a PEM and therefore should only allow the migration of small, positively charged ions. Ferricyanide is neither small nor positively charged and should therefore be blocked by the Nafion membrane from getting to the electrode surface to record a redox signal.

The Donnan exclusion principle states that negatively charged mobile ions will not migrate into a membrane with negatively charged fixed ligands.[17] However, it has been observed that there is some "leakage" of anions into and out of negatively charged membranes.[18]

Unnikrishnan et al. observed “co-ion leakage” in Nafion membranes. They presented one side of a Nafion membrane with a feed solution containing a variety of anions (F^-, Cl^-, NO_2^-, ect.) and had an anion free solution of pure water as the receiving solution on the other side. After a period of time, a aliquot of the receiving solution was tested for the presence of the anions using ion chromatography. They consistently found anions in the receiving solution meaning, there was transport of the anions through the Nafion membrane. Bard and Dewulf took it a step further and performed essentially the same experiment using ferricyanide. The receiving solution was optically monitored for the presence of ferricyanide until its concentration reached 0.11mM. Their experiment lasted almost ten days and they were able to determine the diffusion coefficient for ferricyanide through a Nafion membrane to be $1.9x10^{-8}$ cm^2/s. Literature values for the diffusion coefficient of ferricyanide in bulk soution are generally around $6.5\text{-}7.0x10^{-6}$ cm^2/s.[19-24] The conclusion from these two groups is that anions, including ferricyanide, do get through the Nafion membrane, albiet very slowly.

1.4 HYDODNAMMIC VOLTAMMETRY AT A ROTATING DISK ELECTRODE

The hypothesis is that hydrodynamic voltammetry with ferricyanide as a probe molecule can be used to report tears or loss of integrity of Nafion membranes. Hydrodynamic voltammetry at a rotating disk electrode (RDE) is a simple technique, well-known, and has excellent signal differentiation between diffusion in solution at a bare electrode surface and diffusion through a membrane covering the electrode surface. The last point is essential to our project as this is exactly what will be compared. The time scale of the RDE experiment should be too short for ferricyanide to be observed diffusing through the membrane.

Hydrodynamic fluid convection at a rotating disk electrode (RDE) is shown in Figure 3. The typical three electrode configuration is used with the exception that the working electrode is rotated during the experiment.

Rotation creates a laminar flow across the surface of the disk and continually brings fresh solution and analyte to the electrode. This results in a steady-state current at potentials extreme from the standard potential because the analyte is not being locally depleted. There is a well defined diffusion layer of stagnant solution adjacent to the electrode surface. The thickness of this layer is controlled by the rotation rate of the electrode (Figure 4). The relationship between diffusion layer thickness and rotation rate at a bare electroe is given by Equation 1.2 from Tobias, Eisenburg, and Wilke.[25]

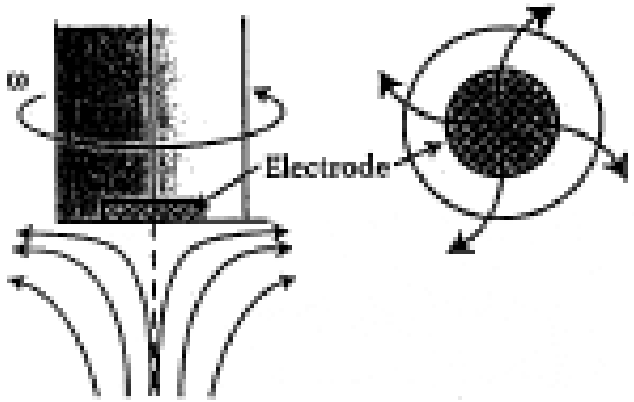

Figure 3. Convection at a rotating disk electrode constantly brings fresh analyte to the electrode surface during experiments.[1, 2]

$$\delta = 0.647 \left(\frac{D}{\nu}\right)^{1/3} \left(\frac{\nu}{\omega}\right)^{1/2} \qquad \textit{Eq. 1.2}$$

where δ is the diffusion layer thickness (cm), D is the diffusion coefficient (cm^2/s), ν is the kinematic viscosity of the fluid (cm^2/s), and ω is the rotation rate (revolutions/s). If in a solution of 5mM ferricyanide in 0.1M KCl the diffusion coefficient is approximately $7x10^{-6}$ cm^2/s and the kinematic viscosity is about 0.01 cm^2/s. Wth these known values we can determine the

theoretical diffusion layer thickness to be in a range betwen 8-44μm at 3000 and 100 RPM, respectively.

When a membrane is added, the analyte now has to diffuse through both the solution diffusion layer and the membrane. However, if the rotation is fast enough, the diffusion layer becomes so thin that the membrane becomes the dominate obstacle for diffusion. The diffusion coefficient observed now becomes an "apparent diffusion coefficient" and can be considered the diffusion coefficient of the analyte through the membrane. Hydrodynamic voltammagrams at

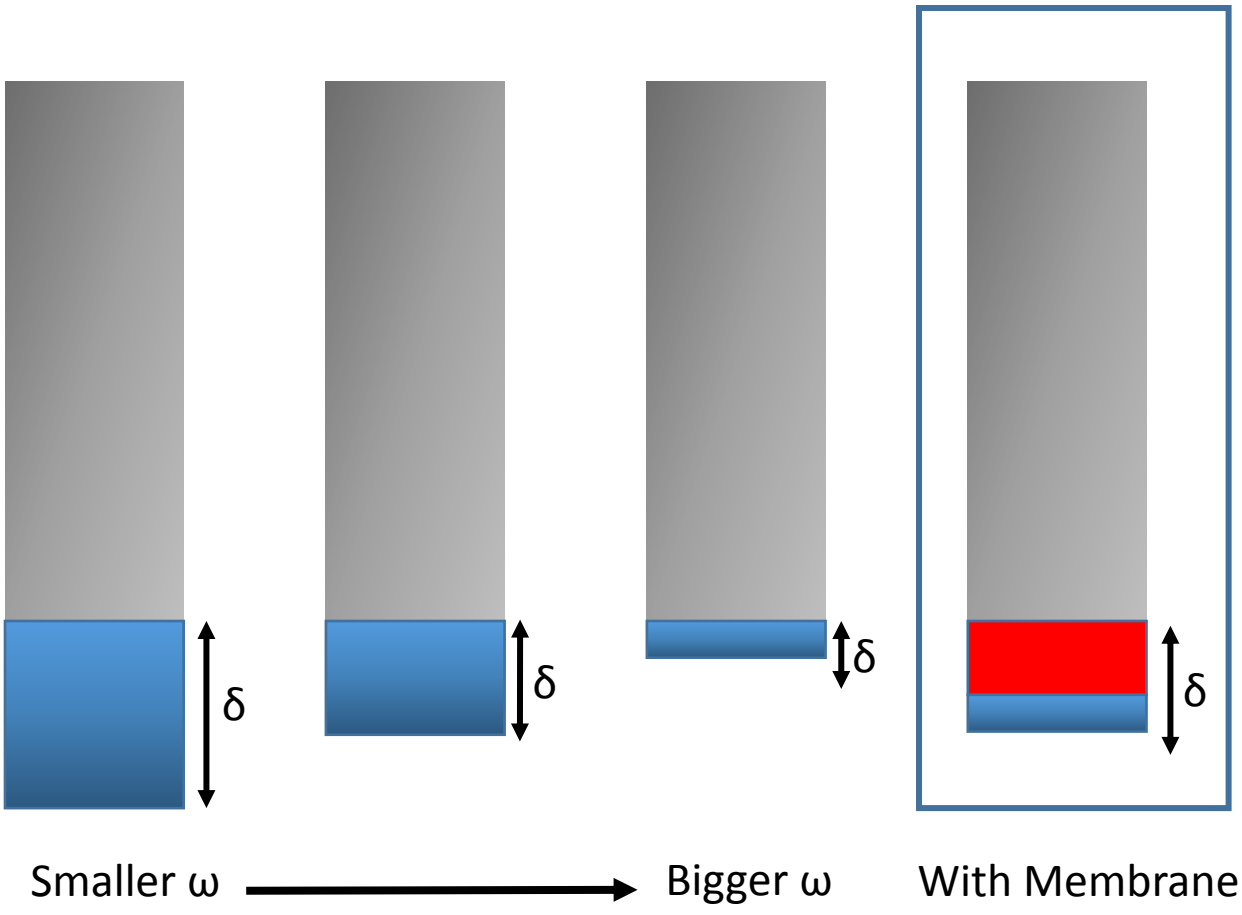

Figure 4. Diffusion layer thickness is controlled by rotation rate. When a membrane is added it has its own diffusional properties that may or may not be related to the rotation rate.

various rotation rates wre used extensively in this thesis to differentiate between solution and membrane transport.

1.5 NAFION MEMBRANE DEGREDATION

This thesis focuses on the integrity of the Nafion membrane. The main failure is caused by the formation or holes or tears in the membrane. Laconti suggested that what little fuel crossover there is in a fuel cell will create hydroxy and hydroperoxy radicals (Figure 5) that will attack the backbone of the polymer membrane creating a small hole. When the membrane is hydrated, and the strain put on the backbone, the hole will propagate into a larger tear. Curtin provided further details explaining that the process starts at a terminal fluorinated carbon on the backbone of the polymer as shown in Figure 6. Due to imperfections in the polymerization process of the membrane, sometimes this type of carbon is not totally fluorinated. Instead, it can have a carboxylic acid or an alcohol function group attached in place of one or more of the fluorines. This is where the radicals proposed by LaConti are theorized to attack. The radical will rip off the carboxylic acid to create carbon dioxide and water leaving a radical on the polymer itself. This polymer radical will then react with another hydroxy or hydroperoxy radical to oxidize the terminal carbon to a carbonyl (creating hydrogen fluoride as a side product). The newly created carbonyl will react with water to create a carboxylic acid (and more hydogen fluoride). In the end, the original carbon is no longer fluorinated, creating a weak spot in the polymer backbone and becoming the site from which a tear can propagate.

Mechanically, once there is a fault or a tear in the Nafion polymer backbone it will continue it enlarge. This can be related to getting a hole in a pair of pantyhose. One small hole or tear in the stockings will create a “runner” that will affect the rest of the garment. The same can

be said for the membrane. A localized fault or tear acts as a small stress point that is weaker than a more perfect portion of the membrane and is therefore more vulnerable to degradation. The tear can spread out from the original stress imperfection to the point that the membrane loses efficiency or falters altogether.[26] This process begins as chemical degradation of the polymer backbone by radical attack and leads to mechanical degradation by creating weak points and eventually holes and tears in the membrane. Figure 7 shows a profile of a Nafion membrane (on a gold substrate) with a tear. The sides of the hole appear thicker than the surrouning membrane. This could be due to a recoil affect of the stressed membrane breaking to create the hole. Tears and holes in the membrane allow the ferricyanide can get through the membrane to the electrode surface as illustrated in Figure 8. This is the main objective of this thesis: to use hydrodynamic voltammetry to compare Nafion covered and bare electrode signals of ferricyanide redox peaks to investigate membrane integrity.

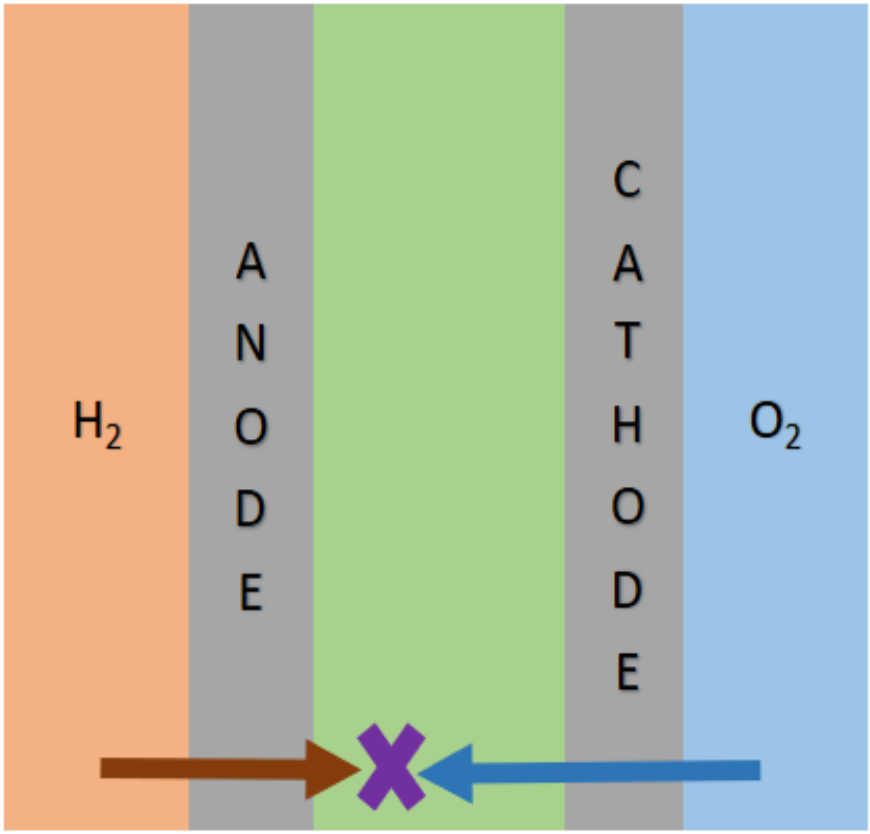

$$H_2 + O_2 \rightarrow H_2O_2$$

$$H_2O_2 \rightarrow \cdot OOH \text{ and } \cdot OH$$

Figure 5. Fuel crossover allows the H_2 and O_2 to react and create hydroxy and hydroperoxy radicals.[7]

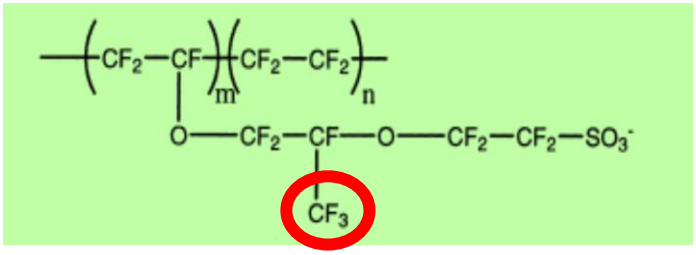

$$R_f - CF_2COOH + {}^{\bullet}OH \rightarrow R_f - CF_2{}^{\bullet} + CO_2 + H_2O \quad (1)$$

$$R_f - CF_2{}^{\bullet} + {}^{\bullet}OH \rightarrow R_f - CF_2OH \rightarrow R_f - COF + HF \quad (2)$$

$$R_f - COF + H_2O \rightarrow R_f - COOH + HF \quad (3)$$

Figure 6. Radicals attack the Nafion polymer backbone at imperfectly fluoronated terminal carbons creating a weakness in the membrane. [2,4]

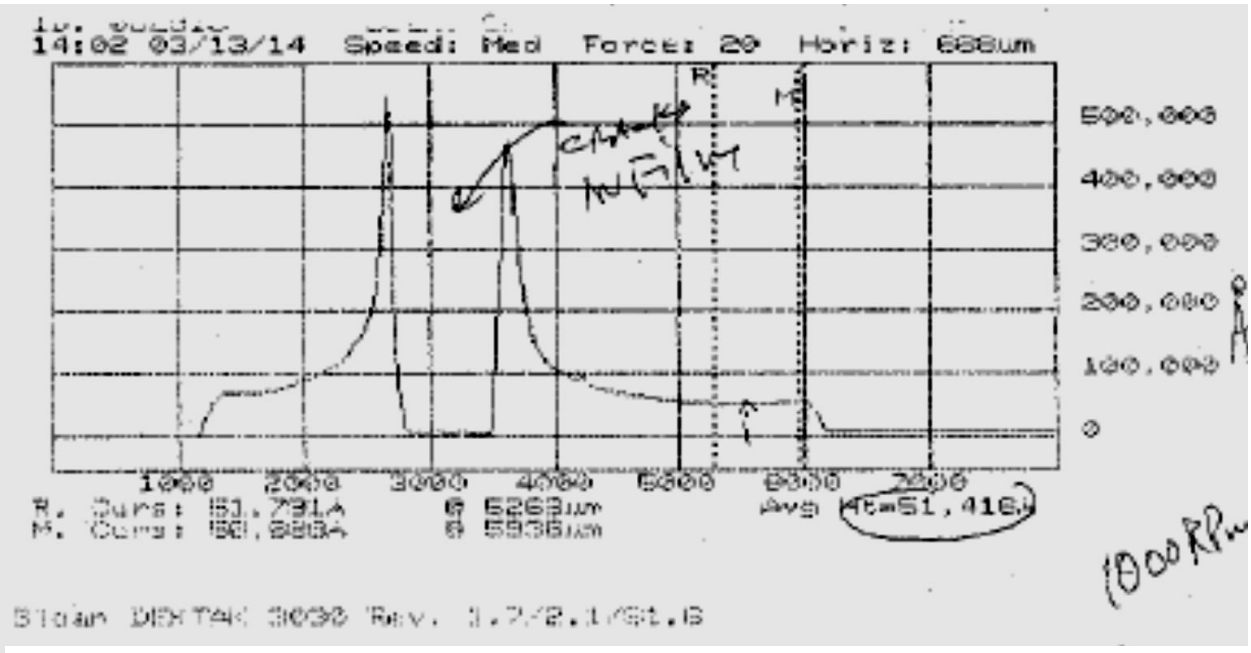

Figure 7. Profile of a compromised Nafion membrane.

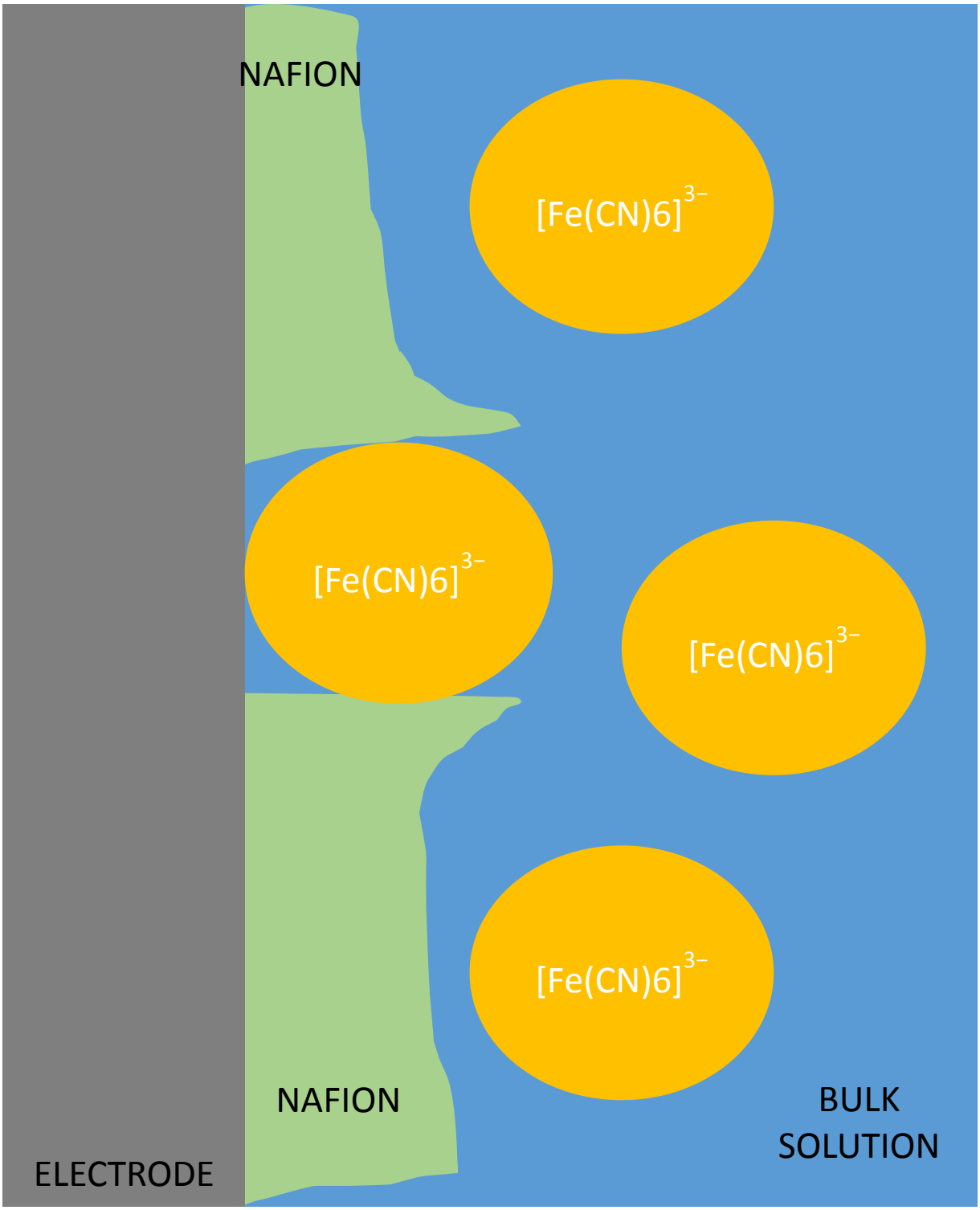

Figure 8. Once there is a tear or hole in the membrane, ferricyanide molecule can reach the electrode surface to generate a signal similar to one generated on a bare electrode.

2 EXPERIMENTAL

2.1 MATERIALS

Electrochemical experiments were performed using a three-electrode configuration composed of a platinum flag counter electrode, a Ag/AgCl in saturated KCl reference electrode, and a 5mm gold rotating disk working electrode (RDE) from Pine Instruments (model AFE6RIPT) and Pine Instruments analytical rotator (model ASR). The working RDE was polished before every use with carbamide 600 grit paper followed by 5, 1, 0.3, and 0.05-micron alumina slurry on a soft pad all from Buehler®. Solutions used included 0.1M KCl (certified ACS grade from EMD Millipore) used to prepare 5mM ferri- and ferrocyanide (solids were certified ACS grade from Fisher Scientific). Kinematic viscosity was determined using a Cannon-Fenske flow viscometer (size 50) from Q Glass Company. The Nafion membranes were recast from the Nafion D-521 dispersion solution 5% w/w in water and propanol obtained from Alfa Aesar.

2.2 MEMBRANE APPLICATION

The Nafion membranes were formed over the RDE by two different methods as shown in Figure 9. The first by drop-casting ten microliters of the Nafion solution onto the center of the inverted electrode surface and allowing it to dry under ambient conditions. The second method was by spin-coating. The same deposition and evaporation steps were used as in drop-casting, but before the drying time began the inverted electrode was rotated at a speed of 1000 RPM for

three minutes. Spinning was seen to spread the Nafion solution across the electrode surface and even slings some of the solution off the electrode entirely.

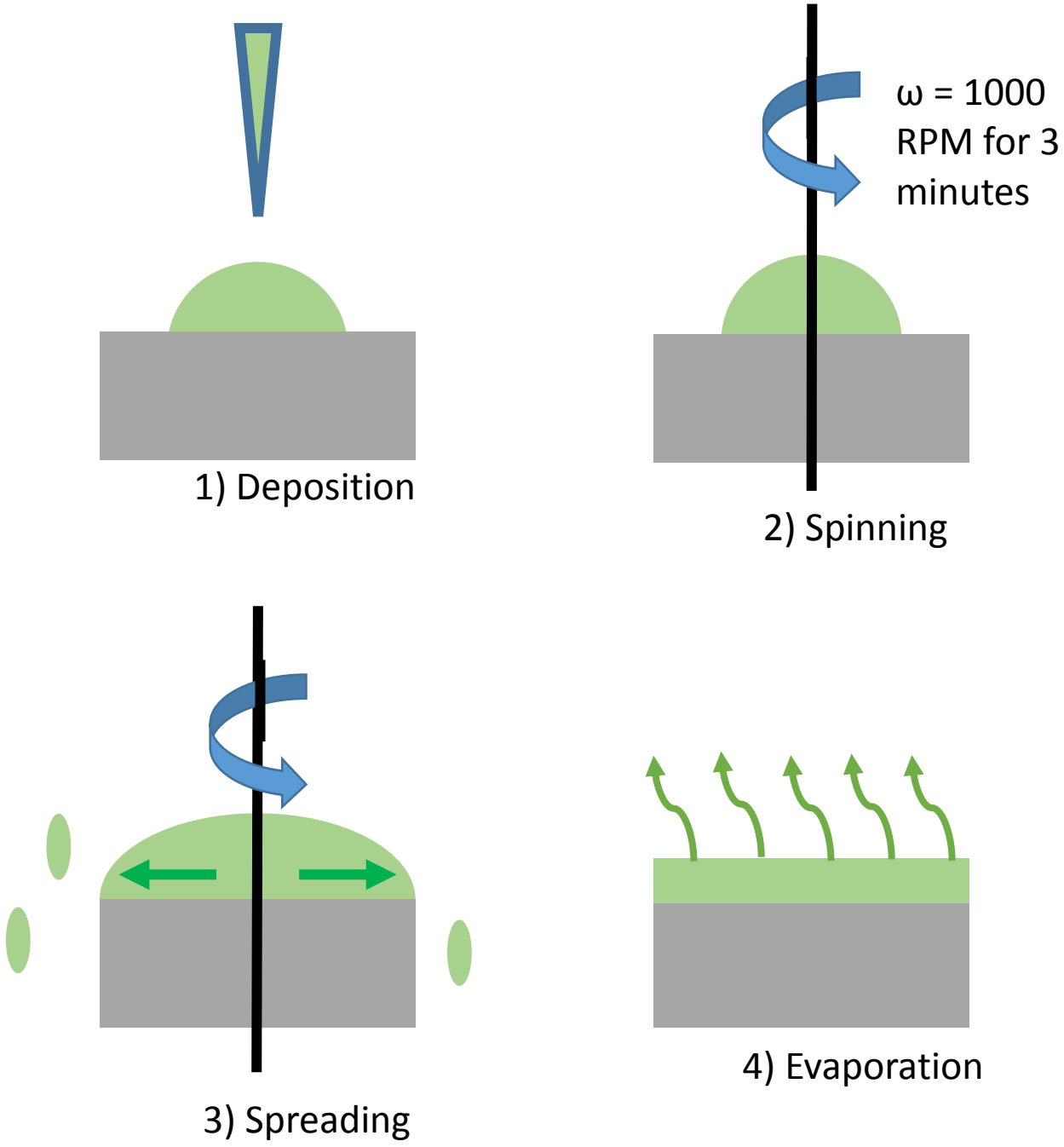

Figure 9. Application of the Nafion membrane was achieved by drop-casting (steps 1 and 4) and by spin-coating (all steps).

2.3 ELECTROCHEMICAL METHODS

For the redox of ferri/ferricyanide, cyclic voltammetry experiments were performed using a CH Instruments 750A potentiostat set to a potential window of +0.5V to -0.1V at a scan rate of 20 mV/s. Rotations rates performed between 100RPM and 3000RPM were controlled with a Pine Instruments rotator and varied throughout individual experiments.

2.4 NAFION MEMBRANE CHARACTERIZATION

The Nafion membrane was evaluated by profilometry with a Dektak 3030 profilometer from Bruker Corporation. Nafion films were spin-coated onto a gold substrate on silicon wafers. The average film thickness was measured and determined to be about 8μm (Figure 7).

A soak study was performed to observe the changes in the redox signal of ferricyanide through a Nafion membrane with differing hydration times. The Nafion membrane was applied to the RDE surface by spin-coating and the membrane was hydrated in 5mM ferricyanide in 0.1M KCl solution for one hour, two hours, three hours, five hours, and overnight (20-24 hours) before performing hydrodynamic voltammetry.

2.5 NAFION MEMBRANE PRETREATMENT

The experiments in this project focused on four different Nafion film pre-treatments. These are outlined in Figure 10. The difference in the pretreatments are the presence of ferricyanide in the hydration solution during soaking and in the hydrodynamic voltammetry solutions. The hydration period (soak time) for the membranes was between 20-24 hours as determined by the soak study discussed later. The membrane treatment in Path A was not soaked in any hydrating solution. The membrane treatment in Path B was soaked in a solution of 0.1M

KCl but the hydrodynamic voltammograms were performed in a 5mM ferricyanide and 0.1M KCl solution. This was the only treatment that did not expose the applied membrane to ferricyanide before performing any cyclic voltammetry. Path C membrane treatment involved a 5mM ferricyanide in 0.1M KCl solution as both the soaking solution and the cyclic voltammetry

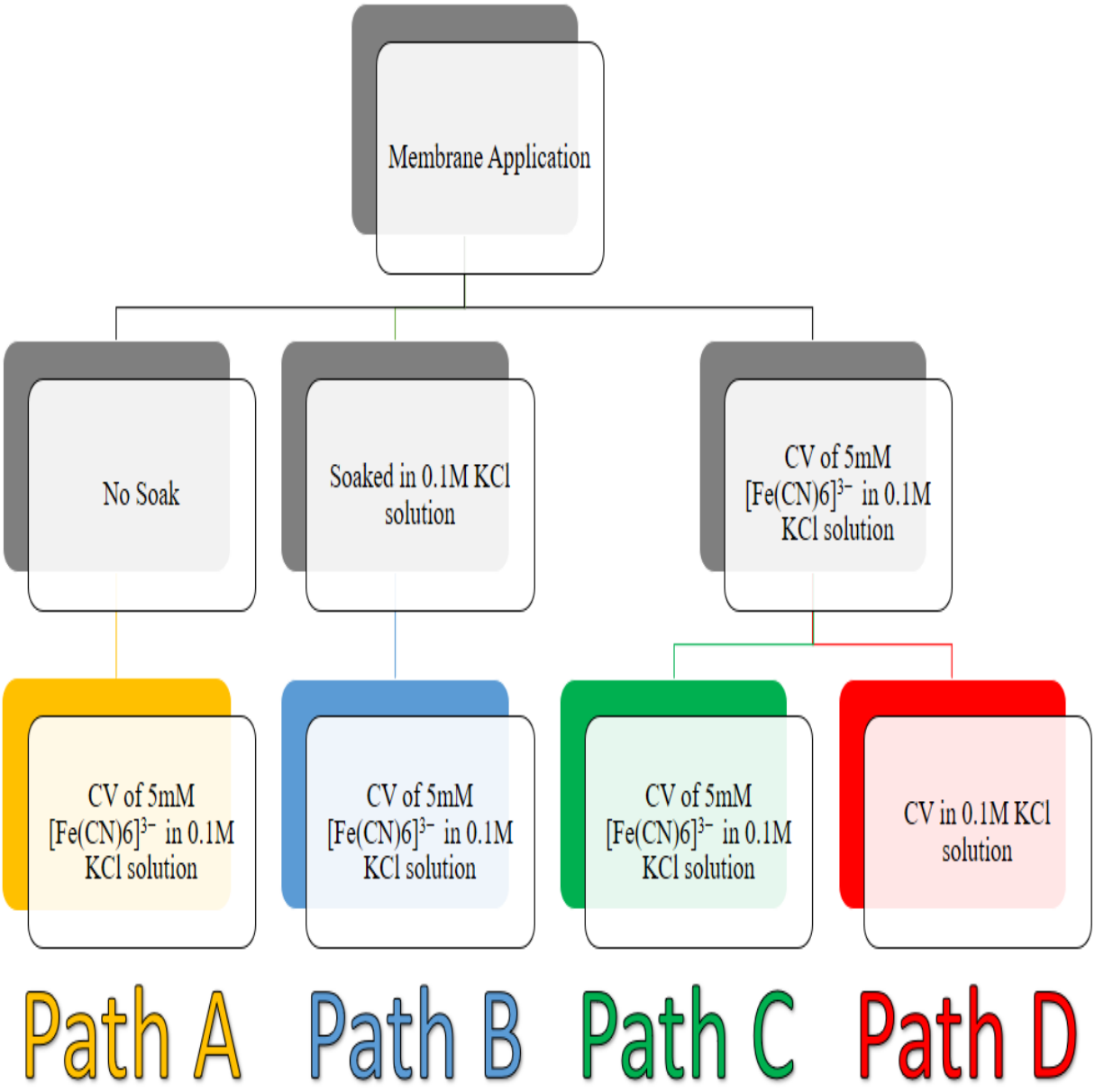

Figure 10. Solutions used for Nafion membrane hydration and cyclic voltammograms.

electrolyte solution. Path D membrane treatment soaked the membrane in 5mM ferricyanide in 0.1M KCl solution but the hydrodynamic voltammograms were performed in only the 0.1M KCl electrolyte solution.

2.6 KINEMATIC VISCOSITY DETERMINATION

The kinematic viscosity was determined by a Cannon-Fenske flow viscometer (size 50) using an average of three trials of the pertinent solutions. The kinematic viscosity was detemined by multiplying the averaged trial times (in seconds) with the viscometer constant at the appropriate temperature with the following equation

$$C = C_O(1 - B(T_t - T_f) \qquad \textit{Eq. 2.1}$$

where C is the viscometer constant, C_O is the known constant at a test temperature, B is the temperature dependence factor, T_t is the test temparature, and T_f is the experimental temperature. The known C_O at 40^{o}C is 0.004311 and at 100^{o}C is 0.004294. This information was used to determine B to be 6.57×10^{-5} and used as the C_O and T_t to determine the actual viscosities. The results can be seen in Table 1.

SOLUTION	AVERAGE TIME (s)	KINEMATIC VISCOSITY (cm^2/s)
Water*	231	0.009953
0.1M KCl	230	0009913
2M NaOH	321	0.013838

*Table 1.Solutions used to determine the kinematic viscosity at 20˚C with the addition of 5Mm ferricyanide. *No ferricyanide added*

2.7 ACTIVE ELECTRODE AREA DETERMINATION

The active area of the electrode was determined by Anson plots. The CH Instrument 750 was used to conduct a chronocolumotry experiment in 5mM ferricyanide in 0.1M KCl. A polished bare gold RDE was used with an applied potential step from +0.5V to 0.0V with a two second pulse width (Figure 11A). The resulting charge observed was used to calculate the actual electroactive area of the electrode from the following equation

$$Q = 2nFACD^{1/2}\pi^{-1/2}t^{1/2} \qquad \textit{Eq. 2.2}$$

where Q is the charge (coulombs), n is the number of electrons in the redox reaction, A is the area of the electrode (cm^2), C is the concentration of the analyte in bulk (mol/cm^3), D is the diffusion coefficient (cm^2/s), and t is the time (s). The charge was plotted against the square root of time (Figure 11B) and the slope was used to determine the active area of the electrode to be 0.21 cm^2. This is about ten percent higher (a roughness factor of 1.1) than the 0.19 cm^2 determined by using the simple geometry equation for a circle

$$A = \pi r^2 \qquad \textit{Eq. 2.3}$$

where r is the radius which is 0.25cm for this particular electrode. The Anson plots are able to account for any rough areas on the surface of the electrode where the geometric equation (Eq. 2.3) can only account for a completely smooth surface.

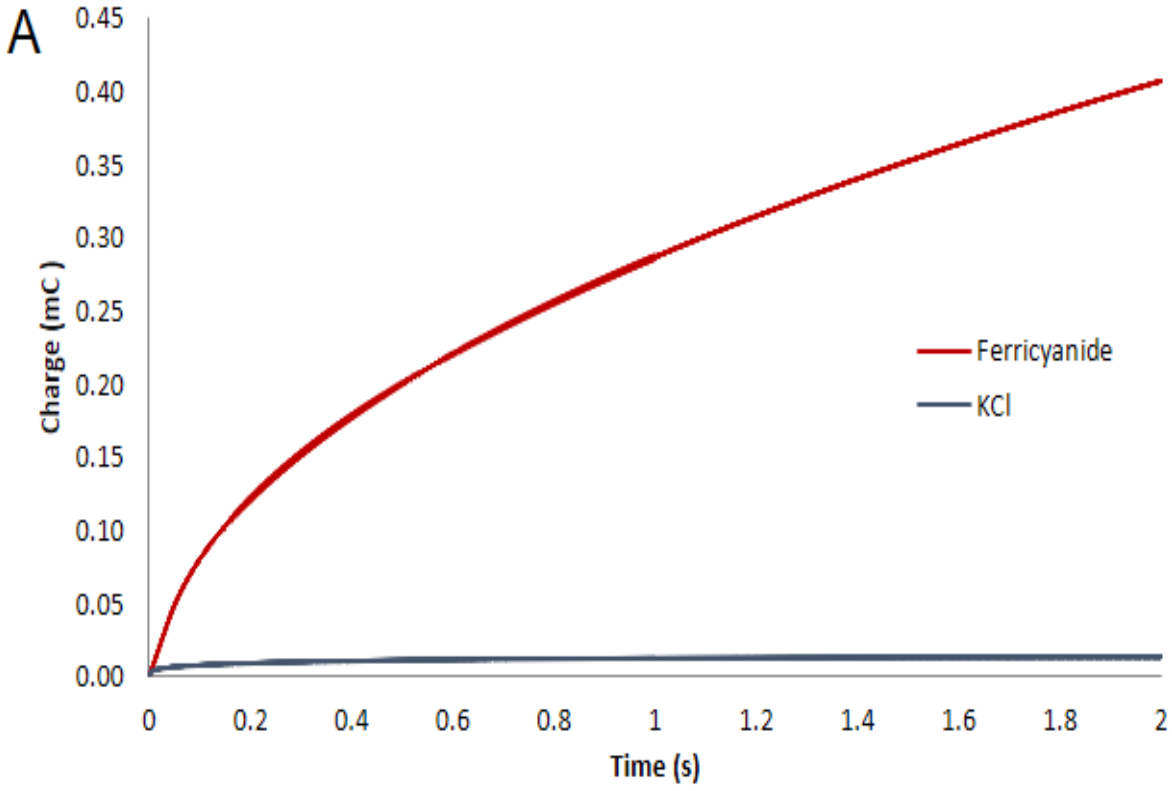

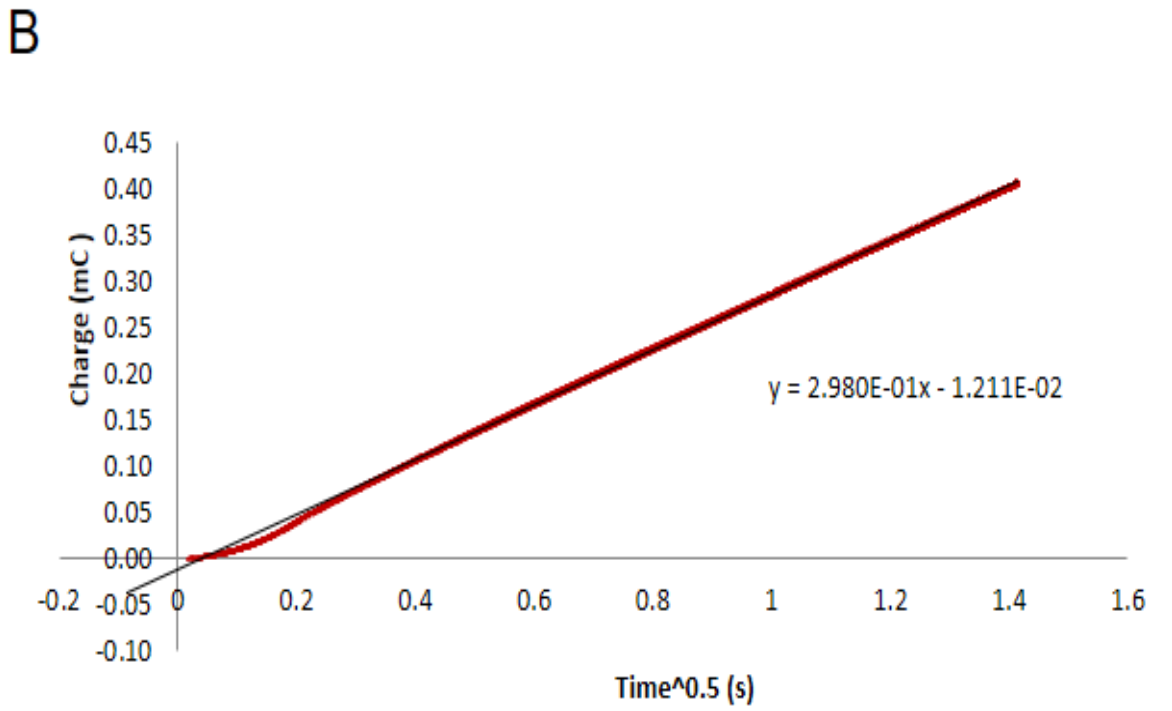

Figure 11. Anson plots used to determine the active area of the bare electrode.

3 FERRICYANIDE AS A PROBE MOLECULE

3.1 HYDRODYNAMIC VOLTAMMETRY

Figure 12 shows the well-known redox peaks of a 50:50 ferri- and ferrocyanide mixture on a bare electrode in bulk solution. This "duck" shape will serve as the diagnostic for later experiments. The idea is that if a "duck" signal is seen then the analyte must be finding bare electrode indicating that the Nafion membrane coverage is incomplete.

Figure 13A shows the hydrodynamic voltammogram for a 5mM ferricyanide solution on a bare gold RDE. At the lowest rotation rates the "duck" shape can still be observed because the diffusion layer is thickest at lower rotation rates (Figure 4) and the analyte is being depleted from the layer. At higher rotation rates, steady-state limiting currents are achieved. This will also be used as a diagnostic for future experiments that contain complications due to the presence of a membrane. Diffusion limited current means that the current is set by the rate the analyte can diffuse to the electrode surface. The bulk diffusion coefficients can be determined using the Levich Equation[27]

$$i_L = 0.62nFAD^{2/3}\nu^{-1/6}C^*\omega^{1/2} \qquad \textit{Eq. 3.1}$$

where i_L is the limiting current (A), n is the number of electrons in the redox reaction (mol-e/mol-C), F is Faraday's constant, A is the area of the electrode (cm^2), D is the diffusion coefficient (cm^2/s), ν is the kinematic viscosity (cm^2/s), C* is the concentration of the analyte in the bulk solution (mol/cm^3), and ω is the rotation rate of the RDE (radians/s). A Levich plot as shown in Figure 13B can be constructed by plotting diffusion limited current against the square root of the rotation rate. The diffusion coefficient can then be determined by the slope of the function if all other variables are known. Analyzing the Levich plot in Figure 13B determined

the diffusion coefficient for 0.2M ferricyanide in 2M NaOH to be $4.68x10^{-6}$ cm^2/s which is within 3% of Eisenburg's $4.54x10^{-6}$ cm^2/s using the same electrolyte.[28]

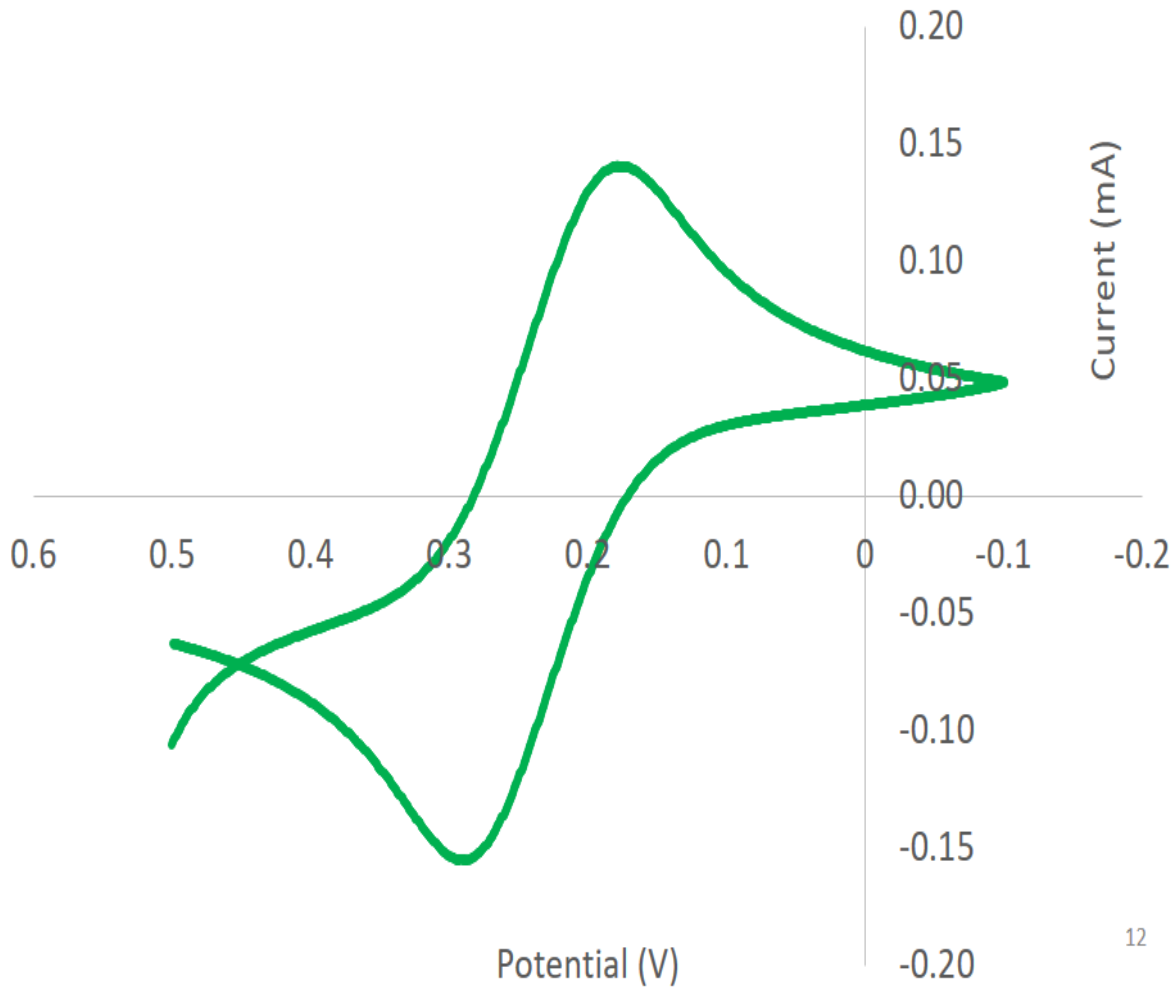

Figure 12. 50:50 Mixture Ferri- and Ferrocyanide Static Signal on Clean Bare Gold Electrode

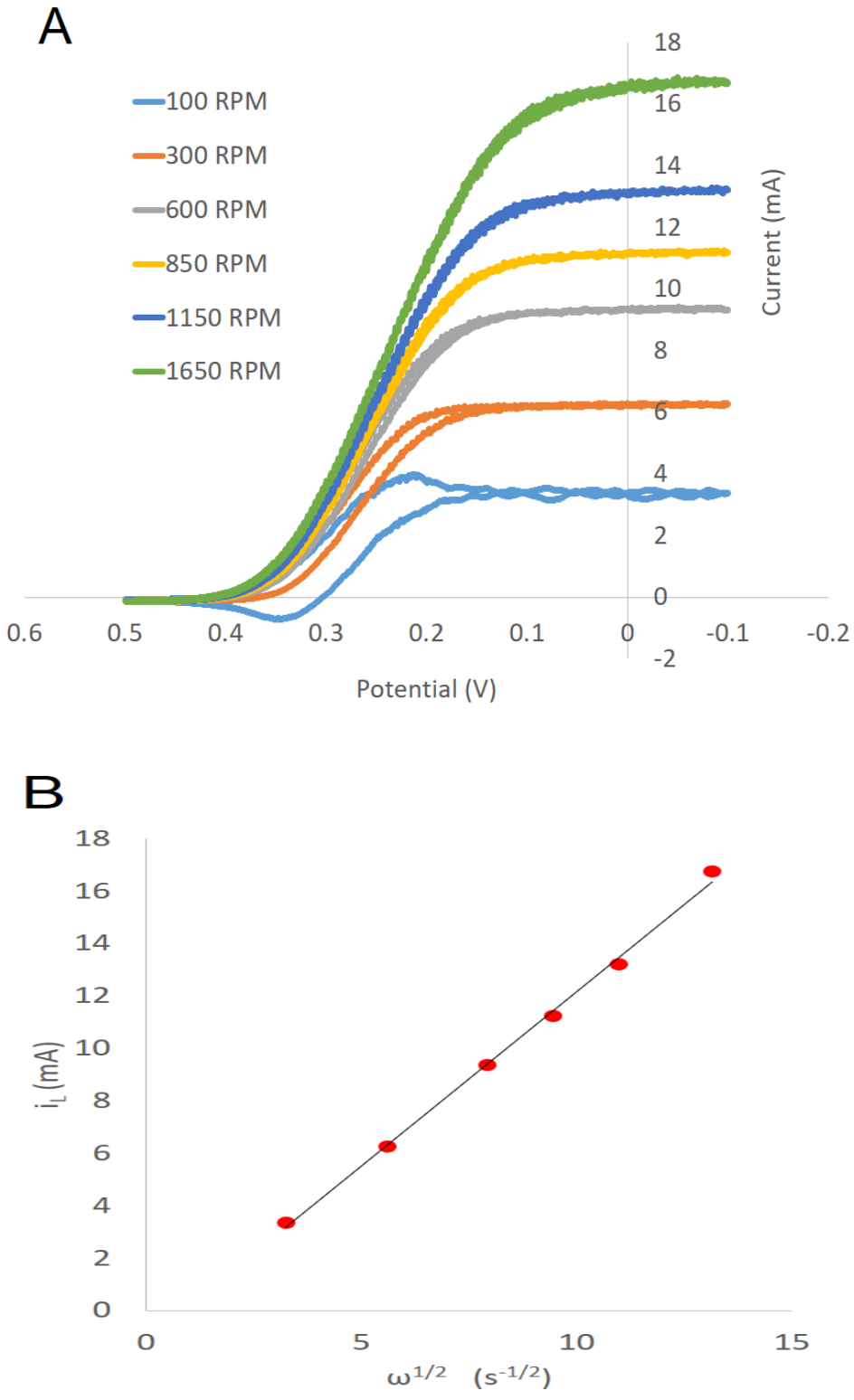

Figure 13. A) 5mM ferricyanide on a bare RDE creates a steady-state diffusion limited signal that can be used to generate a B) Levich plot.

3.2 NAFION COVERAGE

Static cyclic voltammograms were taken of equimolar ferri- and ferro cyanide mixtures on a bare electrode, drop-cast, and spin-coated as shown in Figure 14A. The green curve is the bare electrode. The blue curves are red/ox current for ferricyanide through a drop-cast membrane. There is semblance of a duck shape, but it is distorted when compared to the green curve. With drop-casting, some analyte can reach the electrode surface, indicating there is partial membrane coverage. These curves are not unlike those of unclean or unpolished electrode surface. The red curves are red/ox currents from a spin-coated membrane, showing no ferricyanide signal, and the expected null signal from a complete coating. Essentially, no analyte is getting through the membrane to the electrode surface to create a signal. This comparison shows that spin-coating provides a more complete coverage of the electrode surface than drop-casting. Figure 14B shows the spin-coated red curves on an expanded scale indicating that Nafion completely insulated the electrode. Only a charging current of a few microamps is observed.

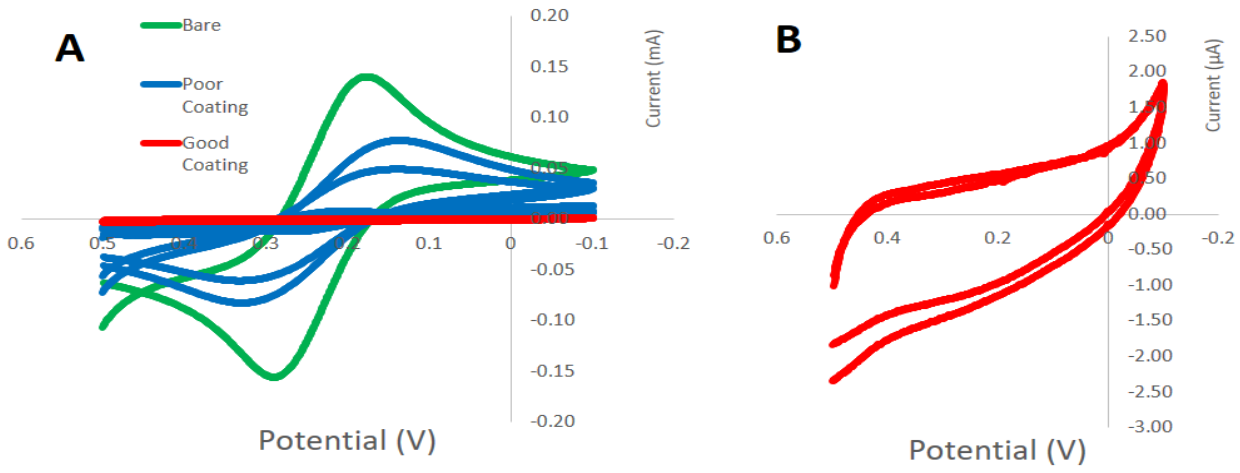

Figure 14. A) Drop-casted membranes (blue) do not reliably or consistently cover the entire electrode surface like a spin-coated membrane does (red). The expanded view of the spin-coated membrane (B) shows only background current indicating that the total electrode surface area is covered because the signal is blocked.

3.3 NAFION HYDRATION

As discussed before, the Nafion membrane must be hydrated to be able to transport ions. The last step in the application of the Nafion membrane is to let the water/propanol solution evaporate which leaves the membrane dehydrated. Therefore, the film must be soaked in electrolyte solution to rehydrate it. A soak study (following Path C from Figure 10) was performed to better understand the hydration limitations and to determine a consistent hydration procedure for future studies. Figure 15 shows a series of voltammograms taken on Nafion coated electrodes with varying soak times. The black curve is a membrane soaked only in KCl. The

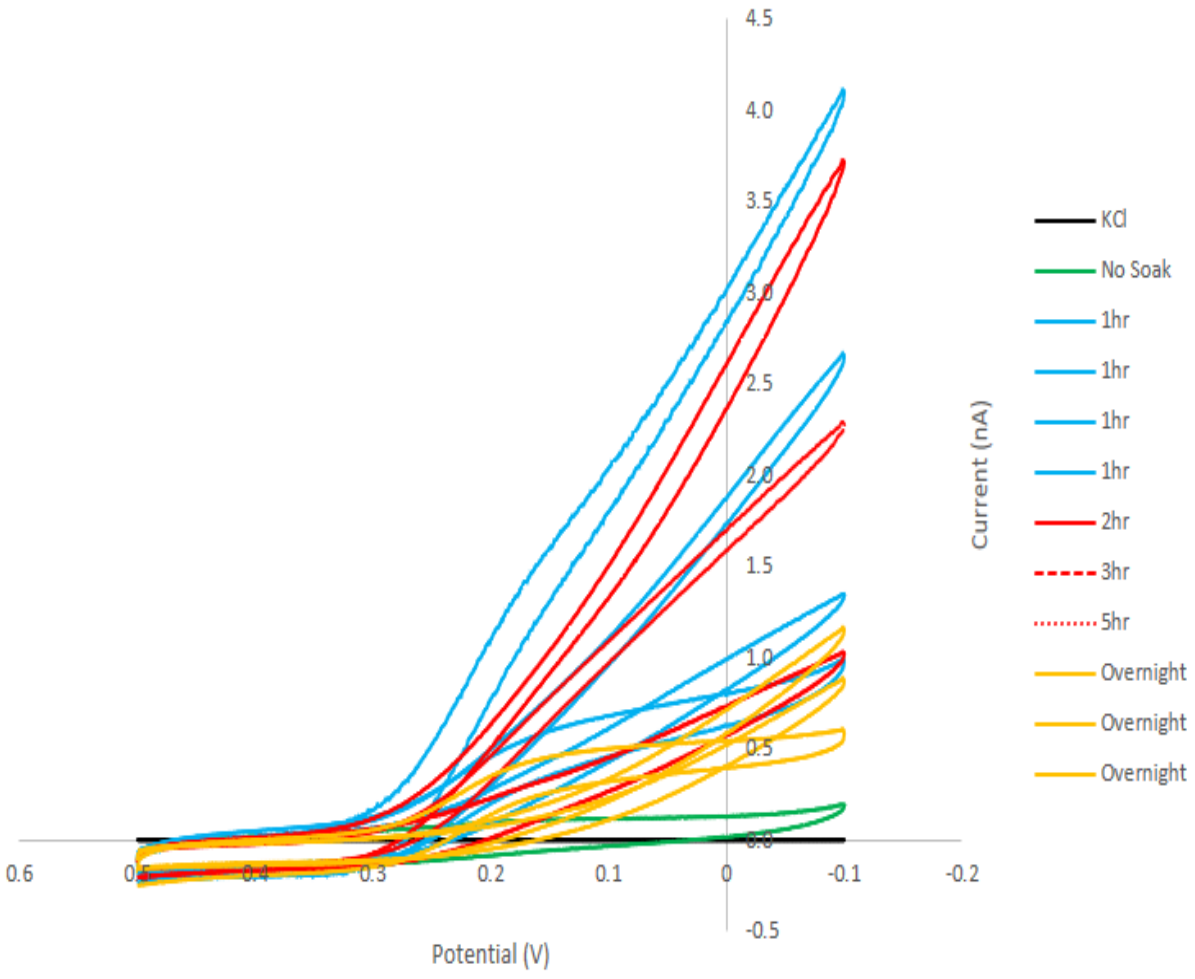

Figure 15. Swelling study of Nafion at 1600RPM in 5mM ferricyanide.

green curve shows a signal from a membrane that has not been hydrated. There is very little current compared to the hydrated curves. The blue curves are signals obtained after the membrane was hydrated for one hour. The signals vary greatly and are not reproducible. The red curves are signals obtained after soaking between two and five hours and are also varied and unreproducible. The yellow curves are signals obtained after soaking for at least 20-24 hours.

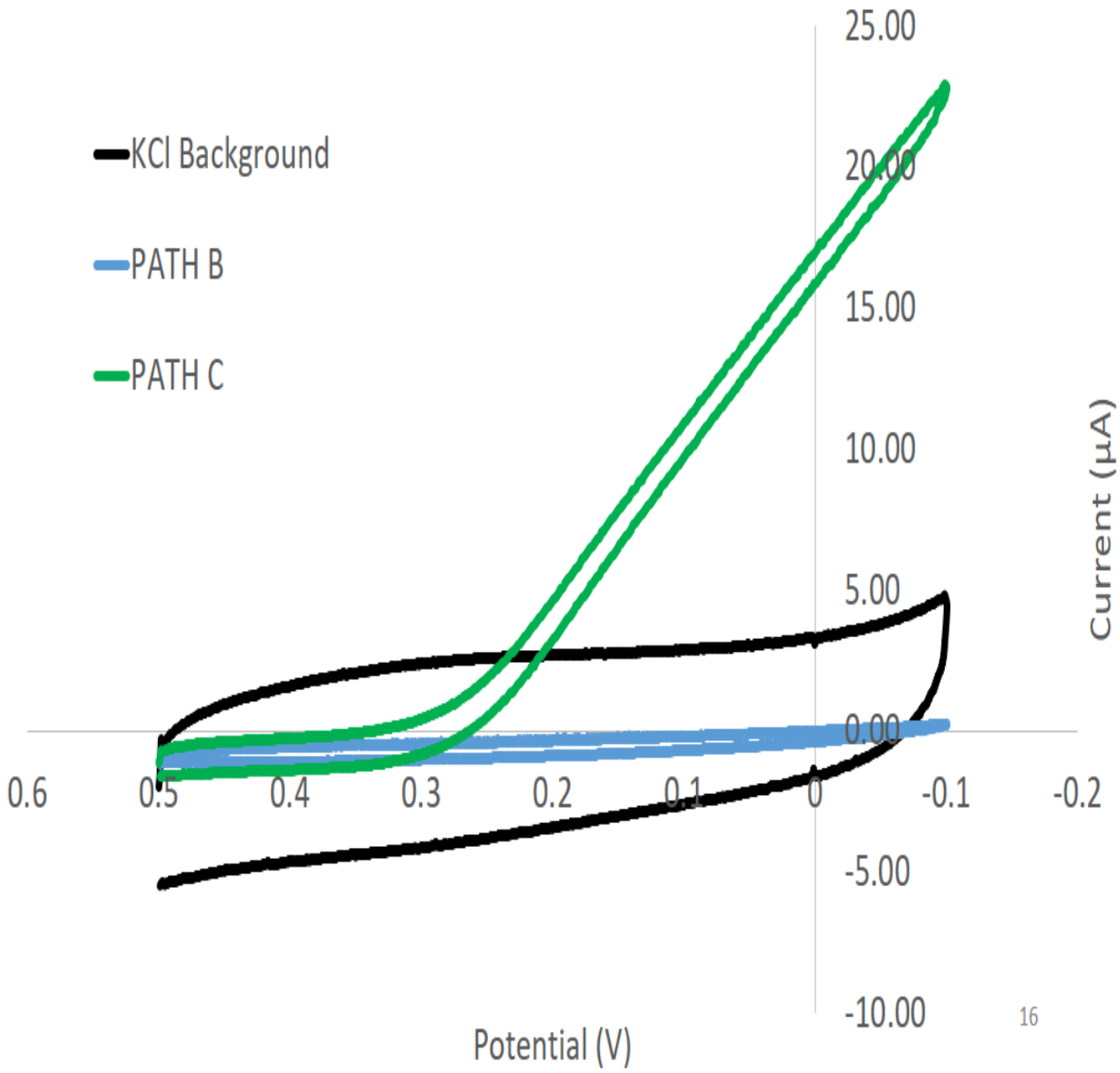

Figure 16. Effects of membrane soaking with and without ferricyanide in the hydrating solution.

These signals are more consistent and reproducible compared to the other soak times. Surprisingly, a current signal from bulk ferricyanide reduction is observed after soaking. More comments on this will be made later.

Figure 16 shows a comparison of Paths B and C to demonstrate the effects of adding ferricyanide to the hydrating electrolyte solution. The black curve is a bare electrode in simple KCl solution. The blue curve is the signal obtained through a spin-coated membrane that was soaked only in electrolyte solution. When compared to the black curve it is obvious that the film is present as there is a 95% collapse in the charging current (5μA to 0.2μA). This is due to Nafion having a much lower dielectric constant approximately 6.28[29] (which is slightly higher than the comparative Teflon at 2.1[30]) compared to the electrolyte solution (bulk water ≈ 80[31]). This is seen in Equation 3.2 where capacitance (C) is directly proportional to the dielectric constant (∈) as well as to the area of the plates (A) and the inverse of the distance between the plates (d)[32].

$$C = \frac{\in A}{d} \qquad \textit{Eq. 3.2}$$

However, when this same type of membrane is soaked in an electrolyte solution containing ferricyanide, a signal is produced (green curve using Path C) that was absent when the ferricyanide was absent in the soaking (blue curve using Path B). This must mean that the ferricyanide entered the membrane during soaking and is playing a role in producing a signal. This begs the questions of whether ferricyanide is in the membrane or not. To answer this question, Path D from Figure 10 was followed and the outcome is shown in Figure 17. The membrane treatment from Path D took the spin-coated Nafion membrane and soaked it in a solution of 5mM ferricyanide and 0.1M KCl but the cyclic voltammetry was performed in an electrolyte solution of only the 0.1M KCl. There is a clear ferricyanide signal seen around 0.2V.

However, as Path D in Figure 10 indicates, there is no ferricyanide present in the electrolyte solution during the cyclic voltammetry experiment. Ferricyanide was only present in the soaking solution. Therefore, the ferricyanide must be incorporating into the film membrane during soaking. The overall magnitude of the current is virtually the same as the background current

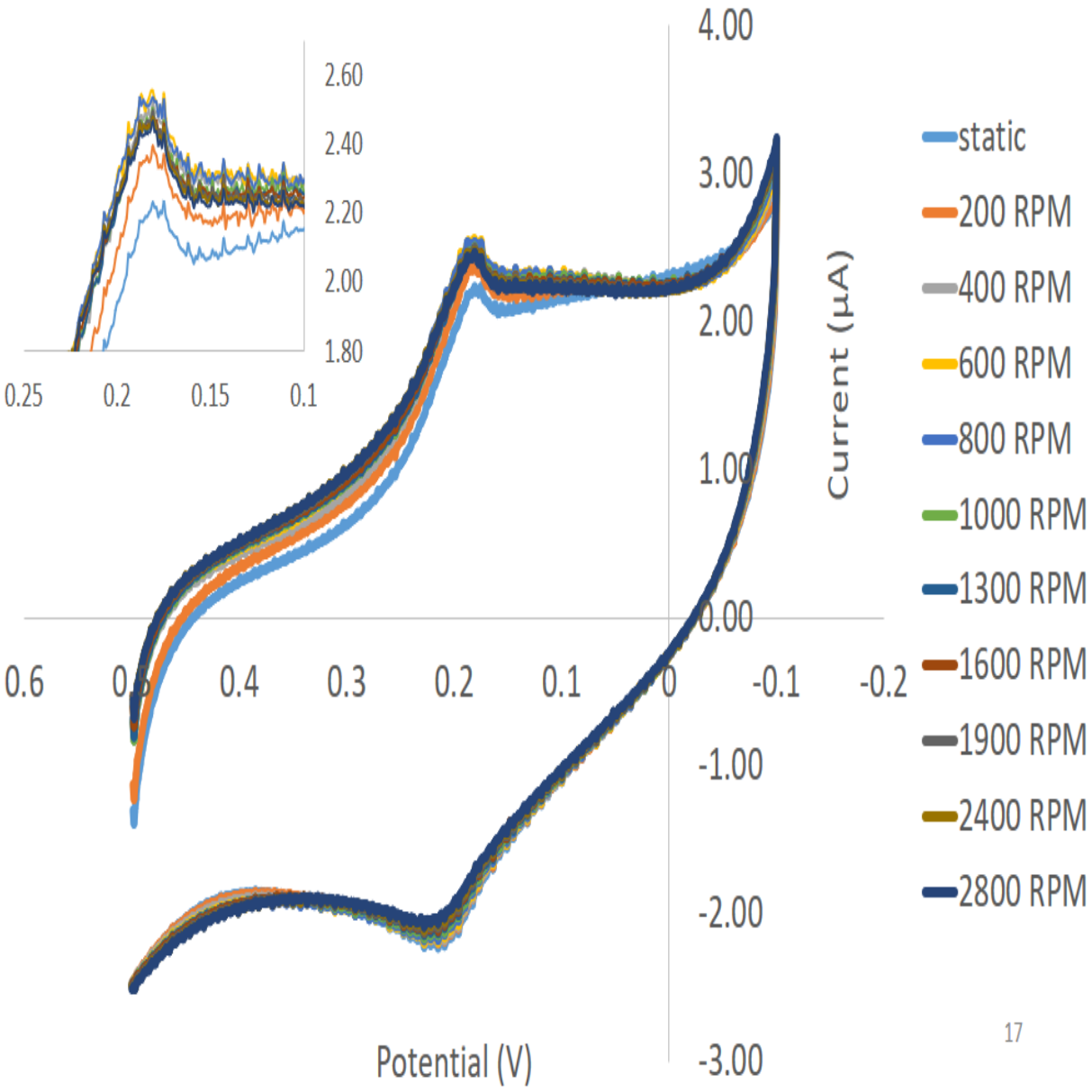

Figure 17. Ferricyanide incorporates into a Nafion membrane (Path D).

seen in Figure 14B, but with the addition of ferricyanide peaks are seen at 0.2V vs Ag/AgCl in saturated KCl reference.

These peaks seem to act as one of two possible cases: thin film or diffusion limited. If a scan rate study had been performed on this film, and the current plotted against the square root of scan rate had produced a linear trendline, then this would have confirmed the thin film theory. One idea is that this thin film could be Prussian Blue, however no color change was observed in the membrane.[33] However, the tailing is still an issue. The tailing observed after the background subtraction is similar to signals seen due to a diffusion limiting factor. This diffusion could be that of the analyte in the bulk, the analyte in the film, or the apparent diffusion of the electrons (to be discussed in later in Section 5 of this thesis). Ferricyanide is absent in the bulk solution used in the hydrodynamic voltammetry experiments meaning the diffusion limited current is not due to ferricyanide in the bulk.

If this diffusion is due to the movement of the analyte the membrane, then the major question now changes from whether or not ferricyanide is present in the membrane but how it is able to incorporate in the first place. The idea is that Nafion is negatively charged at membrane/solution interface (due to the terminal sulfonate groups) and ferricyanide ions are also negatively charged and therefore the two charges will repel each other. However, if either charge is altered then there could be a charge compensation that allows the incorporation of the ferricyanide analyte into the membrane. The first idea is that the membrane itself is neutrally charged. With a pka of 1.6[34] the sulfonate groups will not be protonated in the 0.1M KCl solution

with a pH of almost 7. However, the potassium ions from the electrolyte solution could be acting as the counter ion for the negatively charged sulfonate groups.

The second idea is that the ferricyanide ion is still attached to some potassium ions to make the overall charge neutral. It has been observed by various groups that potassium ferricyanide does not fully ionize in solutions but rather it retains one or two of its potassium ions making the overall charge of the molecule -1 or -2 instead of the fully ionized -3 charge.[35-37] This would not need as much charge compensation within the membrane. The KCl solution itself is used for the charge compensation. If the KCl incorporates into the membrane during hydration as a neutral charge then the chlorine ions can compensate for the ferricyanide ion incorporation. For every ferricyanide ion incorporated into the membrane, three chlorine ions need to migrate back into the bulk solution. However, if the ferricyanide retains one or two potassium ions then the charge compensation needs less than three chlorines and therefore makes the compensation more plausible.

3.4 Estimation of Ferricyanide in Nafion Membrane

To resolve the ferricyanide signal, the background charging current was subtracted so that only the faradaic current is observed. Figure 18 and Equation 3.7 was used to model the double layer charging current that the faradaic signal rides on top of. Equations 3.3-3.5 are from

the circuit shown in Figure 18. Equation 3.6 is the equation in Laplace form before being translated into equation 3.7.

$$i = \frac{E_{APP}}{Z_{Interface}} \qquad \textit{Eq. 3.3}$$

$$E_{APP} = E_{ip} - \nu t \qquad \textit{Eq. 3.4}$$

$$Z_{Interface} = R_N + \frac{X_C R_L}{R_L + X_C} \qquad \textit{Eq. 3.5}$$

$$\bar{\imath} = \frac{E_{ip}\left(s + \frac{1}{R_L C}\right)}{sR_N\left(s + \frac{R_N + R_L}{R_N R_L C}\right)} + \frac{\nu\left(s + \frac{1}{R_L C}\right)}{s^2 R_N\left(s + \frac{R_N + R_L}{R_N R_L C}\right)} \qquad \textit{Eq. 3.6}$$

$$i_o = \frac{-E_{ip}}{R_L + R_N} + \frac{\upsilon t}{R_L + R_N} + \left(\frac{R_L}{R_L + R_N}\right)^2 \upsilon C\left(1 - e^{\frac{-t}{\frac{R_N R_L}{R_L + R_N} C}}\right) \qquad \textit{Eq. 3.7}$$

Where E_{APP} is the applied potential, $Z_{Interface}$ is the resistance, i_o is the current (A), E_{ip} is the initial potential (0.49 V), R_L is the leakage resistance (300KΩ forward scan and 400KΩ backward scan), R_N is the film resistance (12KΩ forward scan and 35KΩ backward scan), ν is the scan rate (20 mV/s), t is the time since the start of the scan (s), and C is the double layer capacitence (80μF). When the correct component values were applied to this, background current was subtracted from the original signal so theoretically the current created by the ferricyande stuck in the film is the only current

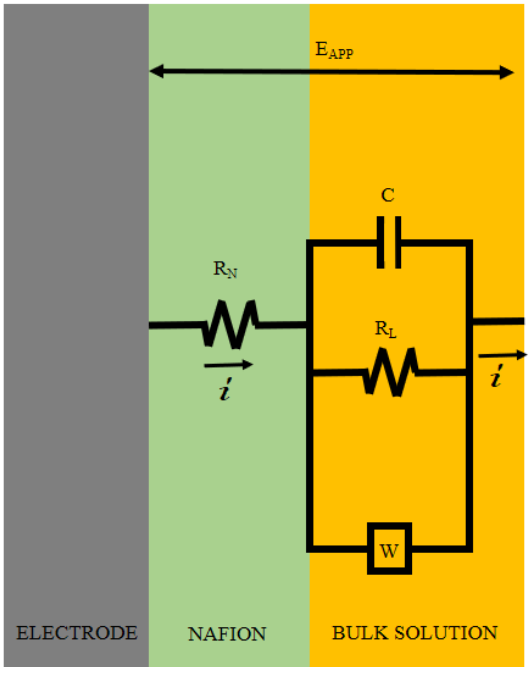

Figure 18. Background Subtraction Modeling Circuit

observed. The background subtracted current can be seen as the grey curve on Figure 19A. This oucome of this subtration plot was expected to mimic a plot from Laviron[6] in Figure 19B. This plot is known as a Frumkin isotherm.[38] If the film is organized with a random distribution of both oxidized and reduced forms of analyte then the i/V curve will be Gaussian. The peak height and width is dependant on the concentration of an adsorbed species, but the peak current consistently occurs at the same potential. However, the plot in Figure 19A, even when corrected for background current, does not appear Gaussian. There is slight peak separation and tailing. According to Smith and White[39], such variables as dielectric constants, analyte concentrations,

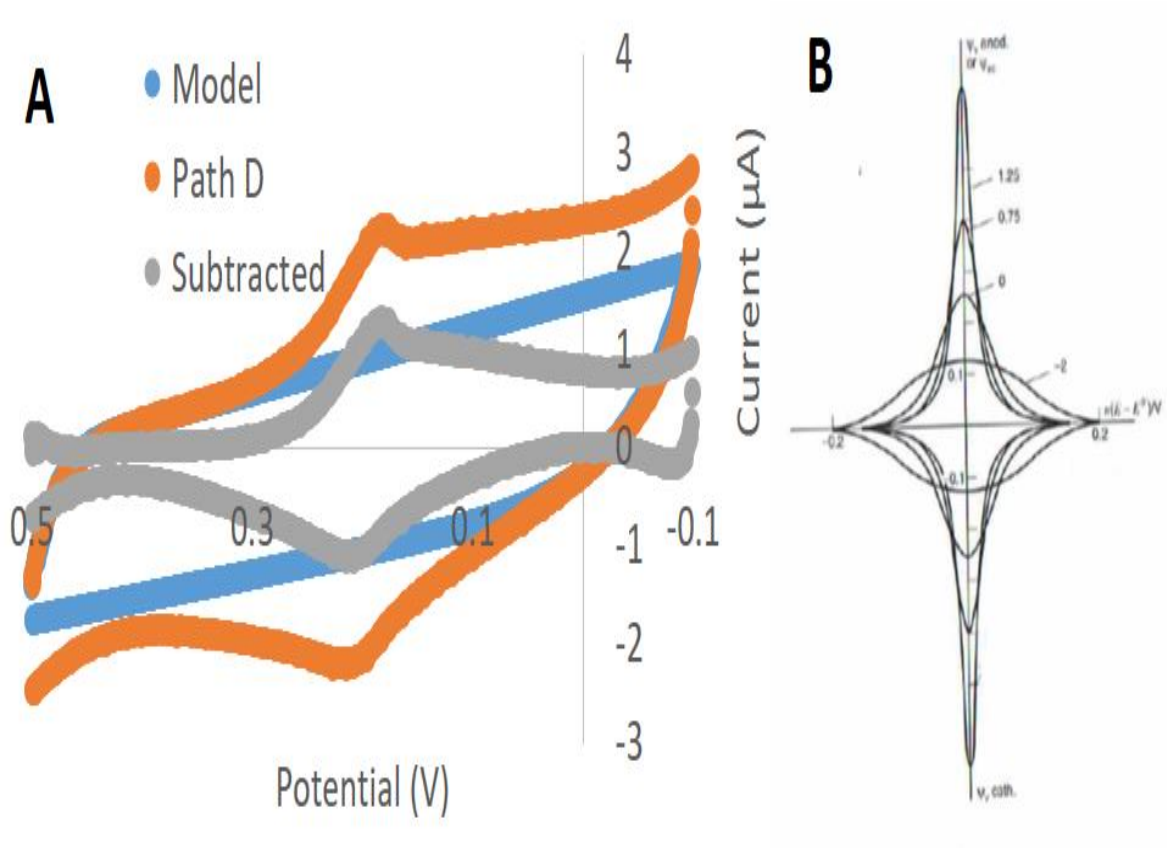

Figure 19. A) Cyclic voltammogram from Path D with background subtraction modeling expected to look B) Gaussian but has tailing due to kinetic properties. [6]

and film thickness can cause the shape of the cyclic voltammogram of adsorbed species to change.

Nevertheless, the corrected plot in Figure 19A with Faraday's law can be used to determine the amount of ferricyanide present in the Nafion film. According to Faraday,

$$m = \left(\frac{Q}{F}\right)\left(\frac{M}{z}\right) \qquad \textit{Eq. 3.8}$$

where m is the mass of the analyte in grams, Q is the charge in coulombs, F is Faraday's constant which is 96485 coulomns per mole, M is the molar mass of the analyte in grams per mole, and z is the stiocheometric number of electrons needed for the reaction to occur. Equation 3.8 can be simplified to

$$n = \frac{Q}{F} \qquad \textit{Eq. 3.9}$$

where n is the number of moles of ferricyanide and z=1 in this specific reaction. To find Q, the background subtracted curve was integrated to find the total amount of charge needed to reduce the ferricyanide trapped in the Nafion. The total charge, Q, found by the integration of this peak was approximately 6μC and the number of moles of analyte was determined to be about 60 picomoles. The membrane is about 8μm thick (from the profilometry data Figure 7) and this mutliplied by the active area of the electrode surface (with a diameter of 5mm) makes the volume of the membrane be 0.15μL. If this volume contains 60 picomoles of ferricyanide the the concentration of ferricyanide is estimated to be 0.4mM within the Nafion membrane. This is less than 10% of the initial bulk soaking solution of 5mM. Additionally, there is no evidence of prussian blue as there was no observable color change in the film. There is a major difference in the cyclic voltammograms of Paths C (Figure 16) and D (Figure 17) that indicates the importance of the components of the bulk solution. When ferricyanide is not present in the bulk

solution the signal shows the analyte being trapped in the film membrane (Figure 17). However, when ferricyanide is added to the bulk solution the cyclic voltammograms appear as in Figure 16 (green curve for Path C) but lacking the limiting current characteristic. This change in signal must be due to the presence of ferricyanide in the bulk solution as all other variables were kept constant.

4 POSSIBLE MECHANISMS FOR ELECTRON TRANSFER KINETICS THROUGH A NAFION MEMBRANE

4.1 DIFFUSION IN THE MEMBRANE

According to the text by Bard[40], there are a few different ways the ferri/ferrocyanide signal redox signal might be obtained through a membrane. The first is by diffusion in the membrane (Figure 20). We discussed earlier how using an RDE creates a laminar flow bringing fresh bulk solution to the electrode surface. If a membrane is present but the diffusion through the membrane is fast, then the redox reaction occurs as if the electrode surface is bare. The rate limiting diffusion factor relies only on how quickly the analyte can reach the outer boundary of the membrane. The Levich Equation (Eq. 3.1) can be applied to the data because the membrane creates no diffusional resistance. This does not describe our system because there is clearly some sort of "resistance" in the diffusion through the membrane. This is obvious when Figures 13 and 15 are compared and the diffusion limited current plateau is achieved on the bare electrode but not the membrane covered.

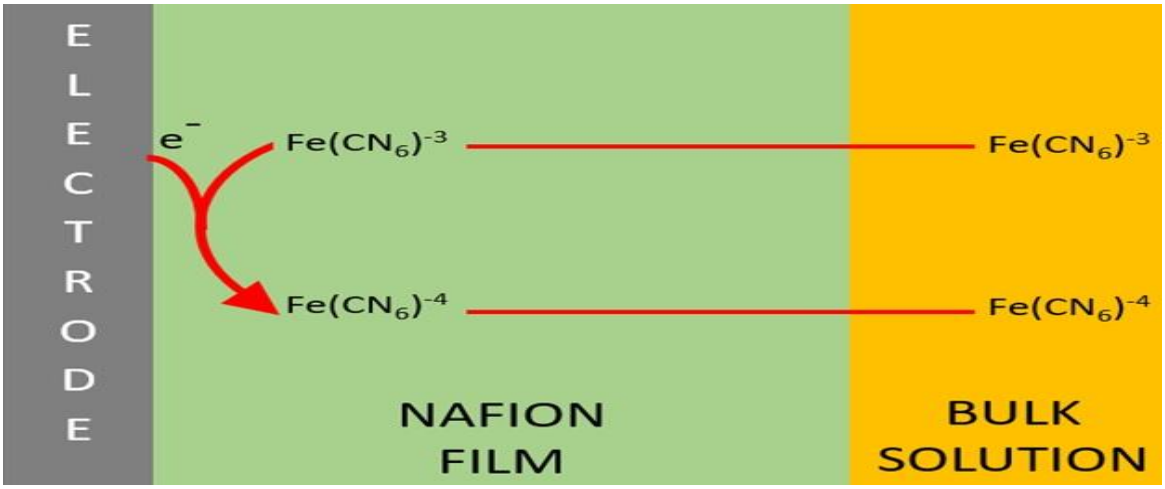

Figure 20. Diffusion through the membrane.

4.2 Cross Reaction Between Analyte and Redox Centers

The second way a signal might be obtained for ferricyanide through the membrane could be a cross-reaction with the analyte and a redox center on the membrane's surface (Figure 21). This is similar to the "lock-and-key model" of enzyme reactions. The idea is that the ferricyanide molecules in the bulk solution will react with the redox centers embedded in the Nafion membrane. Once this reaction has occurred, the electron transfers from the redox center to the ferricyanide molecule, reducing it to ferrocyanide. The redox center is therefore responsible for delivering the charge from the electrode surface through the membrane to the analyte in bulk solution. Assuming there are plenty of electrons available from the electrode, that there are excess redox sites available to react, and that the electron transfer kinetics occur rapidly, the limiting factor in this process is how quickly the actual cross-reaction between a redox center and a ferricyanide molecule can occur. This is similar to our situation because, per Figure 16, we know that the signal requires the presence of ferricyanide in the film. However, it is does not describe our system exactly because both the membrane redox centers and the analyte in bulk solution are the ferri/ferricyanide redox couple and can therefore not react with each other as a cross-reaction.

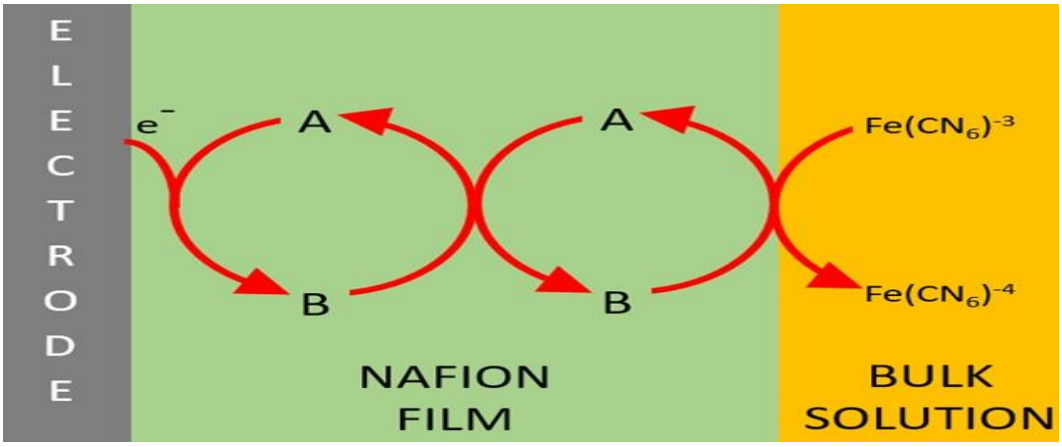

Figure 21. Cross reaction between the analyte and the redox centers within the membrane.

4.3 MEMBRANE LIMITING DIFFUSION

The third possible mechanism could be that the analyte diffuses from the bulk solution into and through the membrane that limits diffusion to the electrode surface (Figure 22). Convection quickly brings the analyte to the membrane surface. The analyte diffuses through the membrane to the electrode surface before it undergoes a redox reaction. If this redox reaction occurs quickly (fast kinetics), then the membrane diffusion coefficient is the limiting factor.

Consider the case where a bare electrode was employed and simple electron kinetics are known to occur. For this particluar project, the ferri/ferrocyanide couple is known to be a reversible reaction (also shown in Figure 12). However, the cyclic voltammograms shown in Figures 15, 16, 18, and 26 (discussed later on) make it look as if the system is irreversible. On a bare electrode, plotting the reciprocals of the current and square root of rotation rate from the Koutecky-Levich Equation (Eq. 4.1) is used to determine the bulk diffusion coefficient found the slope.

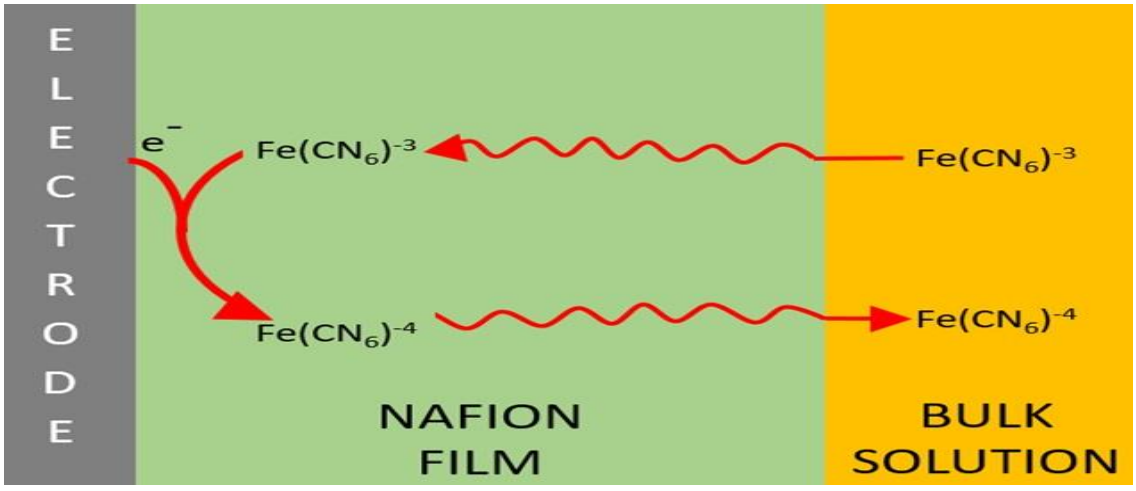

Figure 22. Membrane limiting diffusion of the analyte.

$$\frac{1}{i_d} = \frac{1}{i_L} + \frac{1}{i_K} \qquad \textit{Eq. 4.1}$$

where the diffusion limited current (i_d) is shown to be a composite of the current provided by the Levich Equation (Eq. 3.1) discussed earlier (i_L) and a kinetic variable (i_K) determined by the y-intercept of the Koutecky-Levich plot even without electron transfer kinetics, but instead including properties of the membrane. Because a modified electrode is being used, the equation becomes more complicated. When a membrane is added, Bard's textbook treatment[40] takes the Koutecky-Levich Equation (Eq. 4.1) and provides an explanation for the y-intercept as the sum of the i_m and i_p variables.

$$\frac{1}{i} = \frac{1}{i_L} + \frac{1}{i_m} + \frac{1}{i_p} \qquad \textit{Eq. 4.2}$$

where the total current is the sum the current provided from the Levich flux (i_L), the reactant diffusion current through the membrane (i_m), and the membrane permeation rate given by current (i_p). The maximum current at fast rotation rates (i_m) is dependent on several membrane specific variables.

$$i_m = \frac{nFAD_m\kappa C_A^*}{\delta_m} \qquad \textit{Eq. 4.3}$$

where D_m is the diffusion coefficient of the analyte through the membrane, δ_m is the film thickness, κ is the partition coefficient of the analyte concentration at the inner (φ^-) and the outer (φ^+) boundary of the membrane/solution interface (Figure 23).

$$\kappa = \frac{C_A(\phi^-)}{C_A(\phi^+)} \qquad \textit{Eq. 4.4}$$

Similarly, the i_p is related to the maximum permeation of the analyte into the membrane at the fastest rotation rate.

$$i_p = nFA\chi_f C_A^* \qquad Eq.\ 4.5$$

where χ_f is the rate constant associated with the flux of the analyte from the bulk solution into the membrane in cm/s. This differs from i_m because κ is dependent on the concentration difference of electroactive molecules already inside and outside the membrane while χ_f is the actual rate of movement of those molecules across the solution/membrane interface.

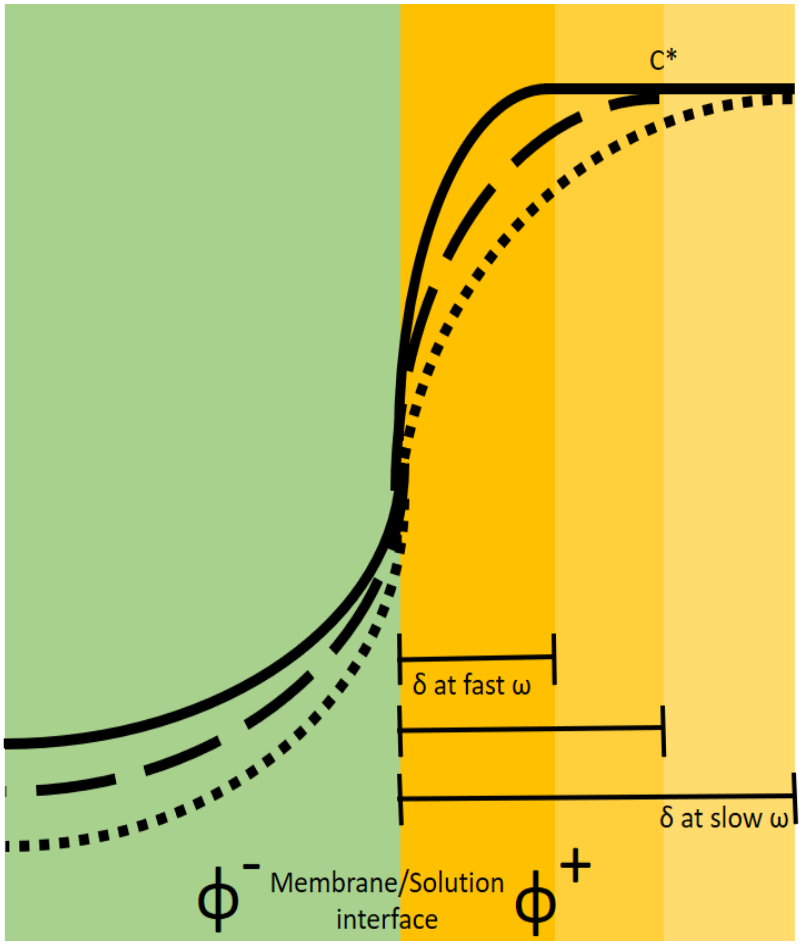

Figure 23. Analyte concentration at the inner and outer boundary of the membrane/solution interface.

However, this exact mechanism is not believed to be the ferri/ferricyanide system being studied in this work. This model is still based on the idea that the analyte can diffuse through the membrane. If this was true for system being studied, there would be no differentiation between Paths B and C (Figures 10 and 16). Instead, a signal (however resistive it is) is only obtained when there is ferricyanide incorporated into the membrane from soaking. When no ferricyanide is present in the membrane, only a background current is obtained.

Gough[41] suggested using permeativity equations that incorporated both the diffusion coefficients for the bulk solution (D) and through the membrane (D_m) and also used the thickness

of the membrane (δ_m), the diffusion layer thickness (δ_d), and the percentage of the analyte concentration in the membrane from the bulk solution (α).

$$i_d = \frac{i_L}{1 + \frac{P_s}{P_m}} \qquad \textit{Eq. 4.6}$$

$$P_s = \frac{D}{\delta_d} \qquad \textit{Eq. 4.7}$$

$$P_m = \frac{\alpha D_m}{\delta_m} \qquad \textit{Eq. 4.8}$$

$$\delta_d = 1.6 D^{1/3} \nu^{1/6} \omega^{-1/2} \qquad \textit{Eq. 4.9}$$

The main issue with Gough's eqations is that diffusion of the analyte through the membrane is still being assumed to be a major contributor to the current signal obtained. This does not fit the model of electron-hopping previously dicussed as the plausible mechanism for the case being studied in this thesis. An equation is needed to determine the apparent diffusion coefficient of the electrons that is also a function of the amount of ferricyanide present in the membrane (the amount of redox centers) as well as an explaination for the rotation rate dependence as seen in later in this chapter.

5 TEDFORD EQUATION

5.1 Overpotential and Scan Rate Study

A full experiment (all rotation rates) following Path C is shown in Figure 24. The lack of diffusion limiting current is due to the resistance of the film. There is also a potential shift where the current begins to increase at 0.4V on bare (Figure 13) to about 0.25V (Figure 24). This is not unlike a low heterogenous electron transfer rate constant which needs a larger overpotential

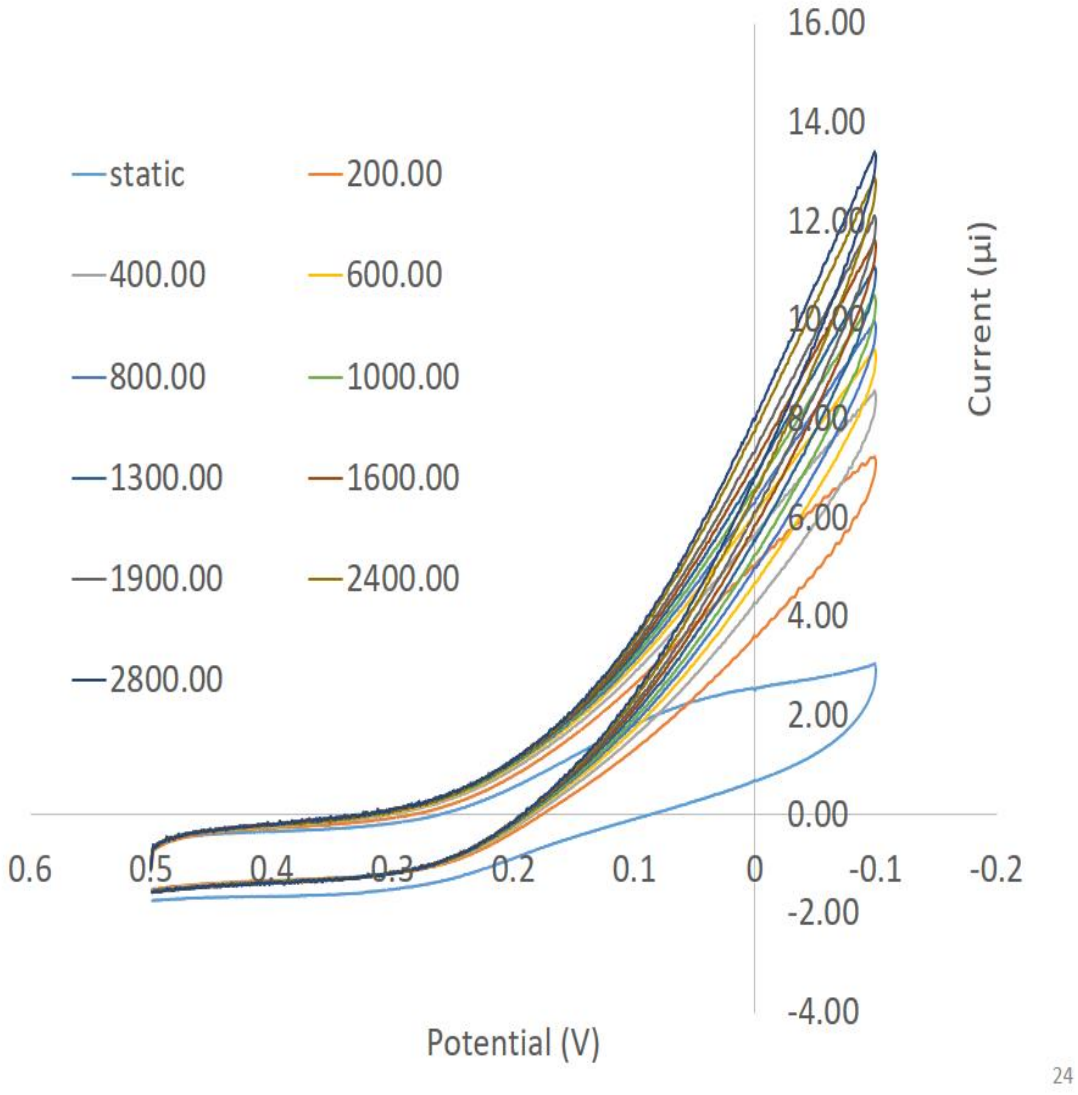

Figure 24. 5mM ferricyanide on a Nafion covered electrode (Path C) with varying rotation rates.

applied to the system before a signal can be obtained. This is seen in Figure 25[5] where case (a) represents a fast rate constant and case (c) represents a situation similar to what is seen in Figure 24. The need for the application of the overpotential could be the result of adsorption of the ferricyanide on the Nafion membrane[38] and the apparent small diffusion coefficient of the electron through the Nafion. However, as larger overpotentials were applied, a diffusional limiting current was never obtained indicating that the resistance is not due

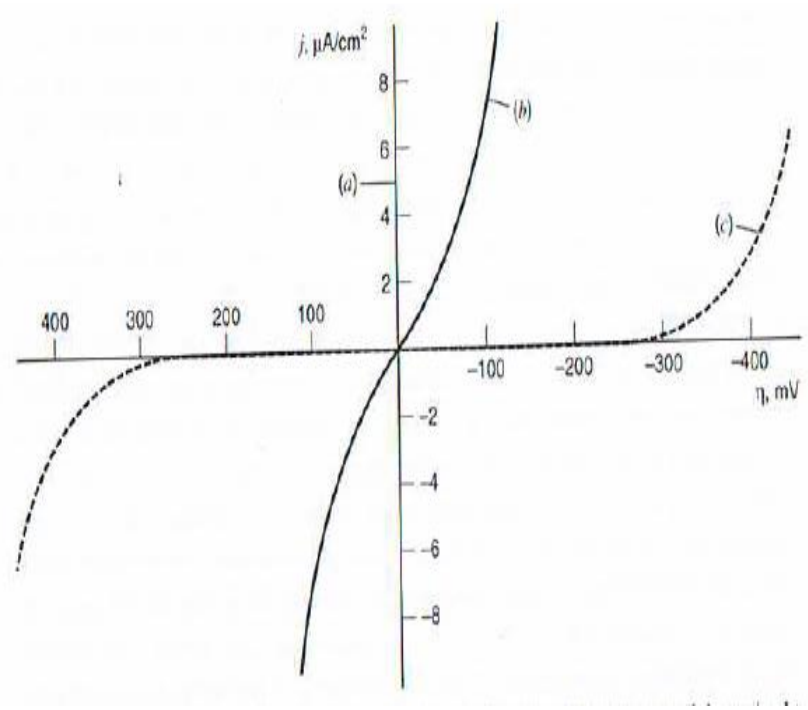

Figure 25. Overpotential can be the result of kinetic properties. Case (a) shows fact kinetics while case (c) shows a slower rate constant.[5]

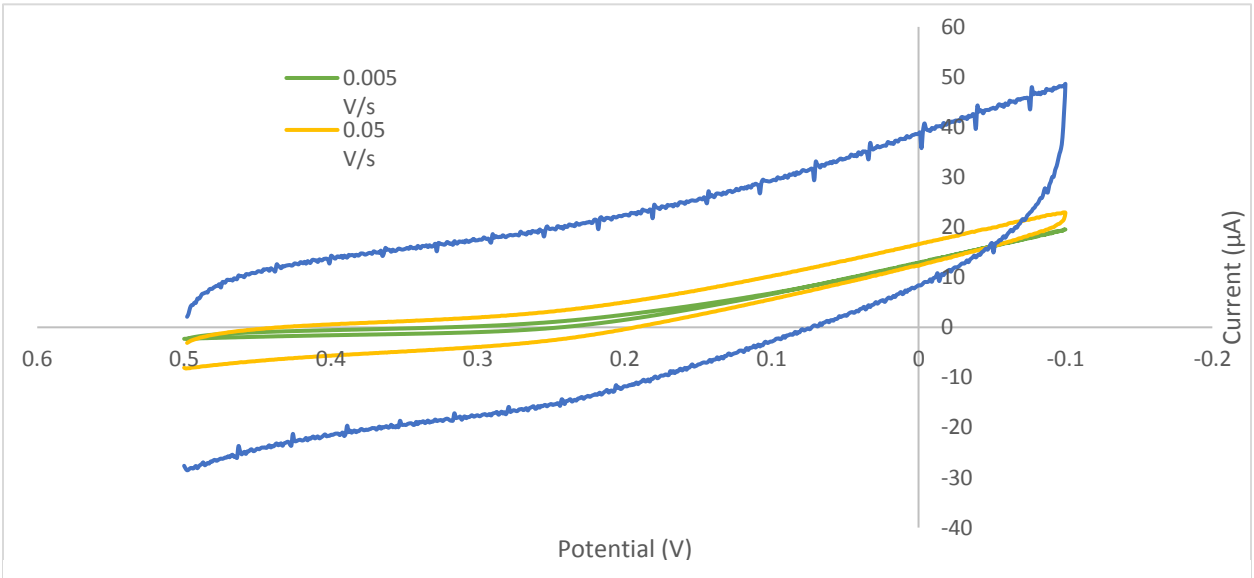

Figure 26. Scan rate study at 1600RPM for 5mM ferricyanide in 0.1MKCl through a Nafion membrane

to slow electron transfer kinetics. Instead, the membrane appears to pass electrons through at a constant impedence.

The scan rate study seen in Figure 26 follows Path C (Figure 10) and also shows that the resistance is not due to electron transfer kinetics. The fastest scan rate shows only a change in the charging current when compared to the two slower scan rates. The shape of the wave is similar to that shown in Figure 24. This indicates further that the resistance observed is not due to slow electron transfer kinetics.

5.2 Apparent Diffusion of Electrons (Electron Hopping)

Because ferricyanide takes a long time to incorporate into the membrane, the diffusion coefficient being observed is the "apparent" diffusion of electrons (instead of the analyte)

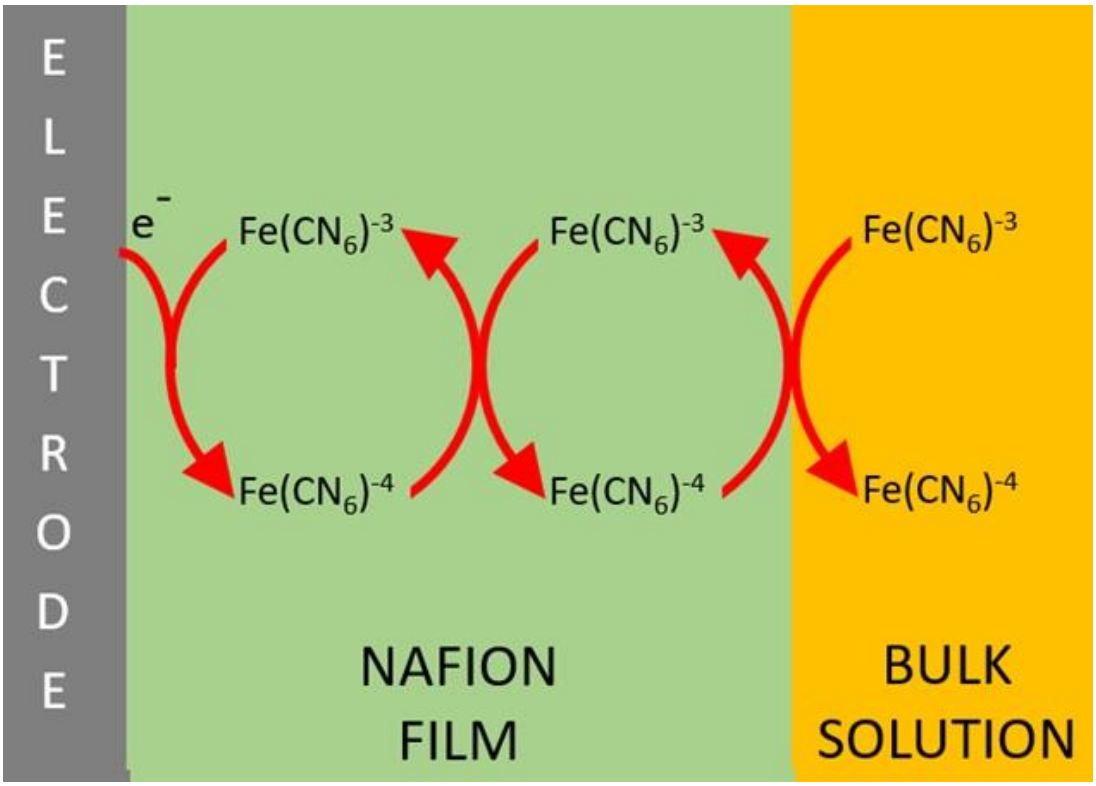

Figure 27. Apparent diffusion of electrons (electron hopping) due to a self-exchange reaction of the redox centers in the film.

through the film (Figure 27). This is an "apparent" diffusion because it is more of an electron-hopping theory rather than actual diffusion of electrons or analyte. The electron from the electrode surface reduces one of the ferricyanide centers in the film to ferrocyanide. It is then used in a redox reaction of another ferricyanide center. This continues until it reaches the membrane/solution interface where the last ferrocyanide in the Nafion membrane reacts with the ferricyanide in bulk solution. This is called a self-exchange electron transfer reaction.[42] This transfer reaction is normally relatively fast because there is no formation or breaking of bonds. This is an outer sphere electron transfer (the electron transfers from one molecule to another without any bonds being formed or broken) and can occur because the products and reactants are the same molecule except for differing oxidation states. The limiting factor in this system is the rate of electron transfer between the redox centers due to the distance between them. The apparent diffusion coefficient of the electron (D_E) can be found using the Dahms-Ruff[43] Equation

$$D_E = D + k\varphi^2 C_p^* \left(\frac{\pi}{4}\right) \qquad \textit{Eq. 5.1}$$

where D is physical movement of the species (assumed in this case to be zero), k is the electron transfer rate constant, φ is the distance between redox sites in the membrane, and C^*_p is the total concentration of both oxidized and reduced redox sites in the membrane. This can then be used to determine the current from the electron diffusion.[40]

$$i_E = \frac{FAD_E C_p^*}{\delta_m} \qquad \textit{Eq. 5.2}$$

Majda[44] states that the two contributions from the redox centers moving and the electrons hopping cannot be differentiated on the sum of a i_E being measured. However, because ferricyanide does not move easily within the membrane, the electron hopping is the more plausible of the two.

Electron hopping is a plausible explanation for the system at-hand because it relies on redox centers in the membrane as seen in the difference cyclic voltammograms obtained with and without ferricyanide in the membrane (Figure 16). Figures 15 and 24 indicate that differing soak times alter the ferricyanide signal obtained. If Equation 5.2 is a correct model, then soak time in ferricyanide directly correlates to the amount of ferricyanide within the Nafion film. The shorter soak times should have less ferricyanide in the membrane so that the average distance between redox sites (φ) will be greater. The longer soak times should have more ferricyanide and a shorter average distance between redox sites. The farther the electron must "hop" between sites, the greater the resistance.

5.3 Using the Levich Plot to Determine Apparent Diffusion Coeffients

Figure 28A shows four Levich plots of ferricyanide: a bare RDE (data from Figure 13A), through a Nafion membrane (Following Paths B and C), and the theoretical curve generated using known values in the Levich Equation (Eq. 3.1) and solving for the current. Other than the application of the Nafion membrane, the only difference is that the bare electrode data was in NaOH electrolyte where as the Nafion covered electrodes were in KCl. The predicted Levich plots for a bare electrode in NaOH and in KCl only differed by 5% allowing the the comparison of the plots to continue to be used. The bare (blue) and theoretical (red) are very similar and creates confidence in the methods being used. The signals through the Nafion with the Paths B and C (Figure 10) pretreated membranes create virtually horizontal lines (gray and green, respectively) when compared to the slope of a Levich line at a bare electrode. When the curve has no slope it indicates that the signal is not diffusion controlled. In this case, the resistance of the membrane is the limiting factor. The difference in the slopes of the bare/theoretical and the

Nafion covered trials can also be explained by the active electrode area. The active area is greatly diminished when the Nafion membrane is applied and therefore the slope (which is directly proportional to A) is also decreased.

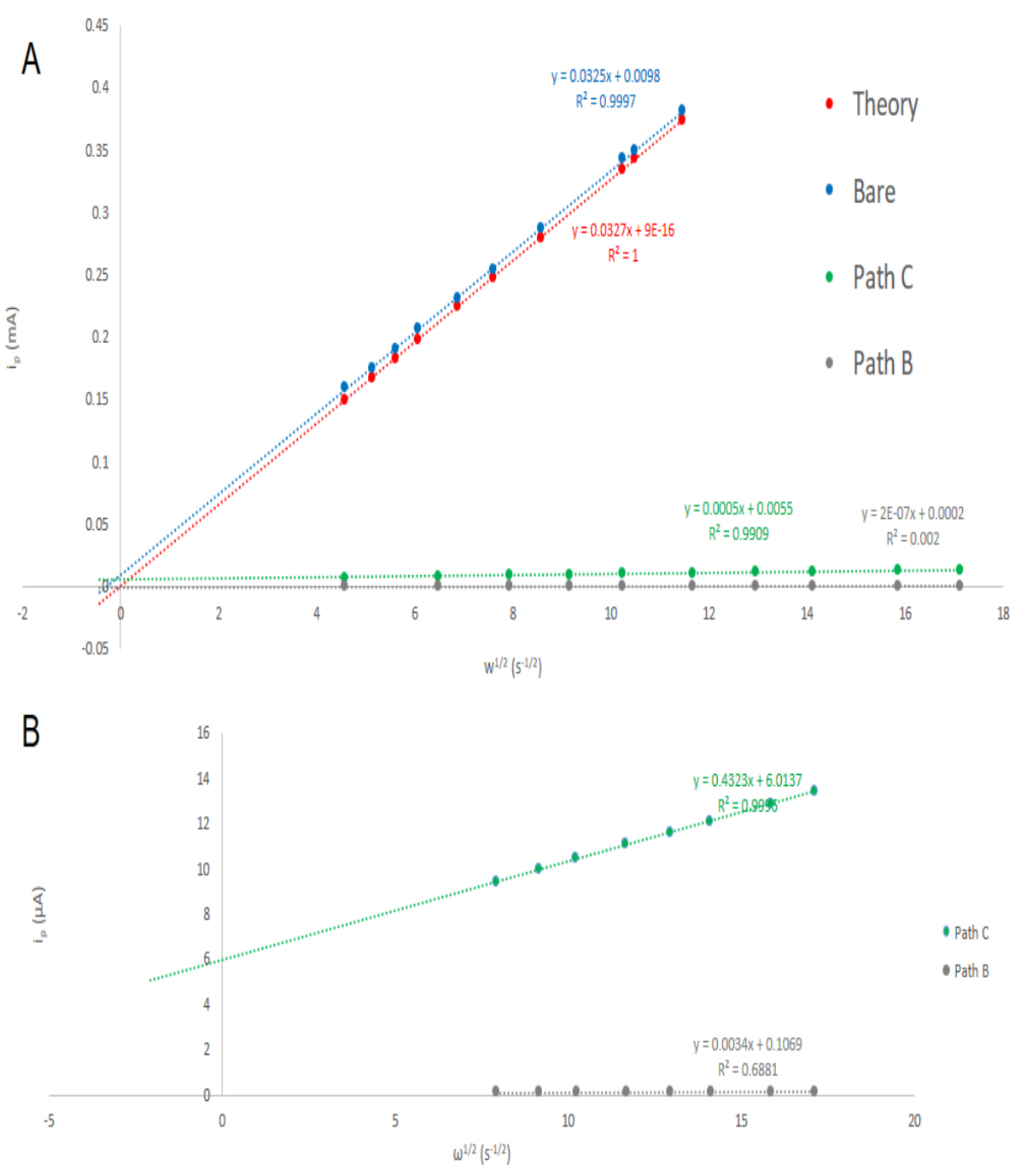

Figure 28, The intercept of the Levich plot can be used in the Tedford Equation to determine a D_E. The Nafion impeded signal looks virtually horizontal (A) compared to a bare electrode until its axis is expanded (B).

The expanded view of the Nafion covered trials (Figure 28B) shows that there is some dependence on the rotation rate so there are some diffusional properties. However, the dependence is miniscule with a slope of only half a microamp per $s^{1/2}$ and observable only when ferricyanide is present both incorporated into the membrane and in the bulk solution.

5.4 USING THE TEDFORD EQUATION

Taking into consideration all the plausible mechanisms discussed in this thesis, an equation was formulated to account for the apparent electron diffusion coefficient and the amount of ferricyanide present in the membrane and bulk solution. This equation is based on the Levich Equation (Eq. 3.1) to account for the intercept observed

$$i_p = i_s + i_E \qquad \textit{Eq. 5.3}$$

where i_p is the peak current (because a diffusion limiting current is never obtained) and is the summation of the current from the solution (i_s) and from the membrane (i_E) with an apparent diffusion coefficient.

The i_s is approximated by:

$$i_s = nFAD\frac{dC}{dx} = nFAD\left(\frac{C^* - C_m}{\delta_d}\right) \qquad \textit{Eq. 5.4}$$

where n is the stoicheometric number of electrons, F is Faraday's constant, A is the active area of the electrode, D is the diffusion coefficient in bulk, C* is the concentration of the analyte in bulk

solution, C_m is the concentration of the analyte that has been incorporated into the membrane, and δ is the diffusion layer thickness in bulk (Eq 4.9).

The i_m is determined by the Equation 5.2 (rewritten here)

$$i_E = \frac{nFAD_E C_m}{\delta_m} \qquad \textit{Eq. 5.5}$$

where D_E is the apparent diffusion coefficient due to the electron-hopping mechanism and δ_m is the thickness of the membrane.

Combining Equations 5.4 and 5.5, the Tedford Equation can be written as the following.

$$i_p = 0.62nFAD^{2/3}\upsilon^{-1/6}\omega^{1/2}(C^* - C_m) + \frac{nFAD_E C_m}{\delta_m} \qquad \textit{Eq. 5.6}$$

Because the diffusion layer thickness (δ_d) contains the rotation rate (ω) as seen in Equation 4.9, the Levich plot of current versus the square root of rotation rate can still be employed. If the intercept from Figure 28B is set equal to the intercept portion of the Tedford Equation (Eq. 5.6), the D_E is determined to be approximately 1.24×10^{-8} cm^2/s. This is logically much slower than that of the literature value solution diffusion value of 7×10^{-6} cm^2/s but is on the same order of magnitude as Bard and Dewulf's[45] 1.9×10^{-8} cm^2/s observed in their experiments using a different Nafion membrane (Nafion 117).

5.5 Using D_E to Compare Different Nafion Films in Various Hydration States

Figure 29 shows Tedford plots for ferricyanide signals through Nafion membranes with various soak times. The intercept of these plots is used with the Tedford Equation (Eq. 5.6) to determine the D_E for different Nafion hydration times. The results can be seen in Figure 30. Figure 29 plots include the bare electrode signal for comparison (A) and show the expanded the scale for a comparison of how hydration time affects the membrane (B). The D_E determined for

the bare electrode is two orders of magnitude higher than those through the Nafion membrane. This is on the same scale as discussed in section 5.4 when comparing the literature values to the experimental and to Bard and Dewulf.[45]

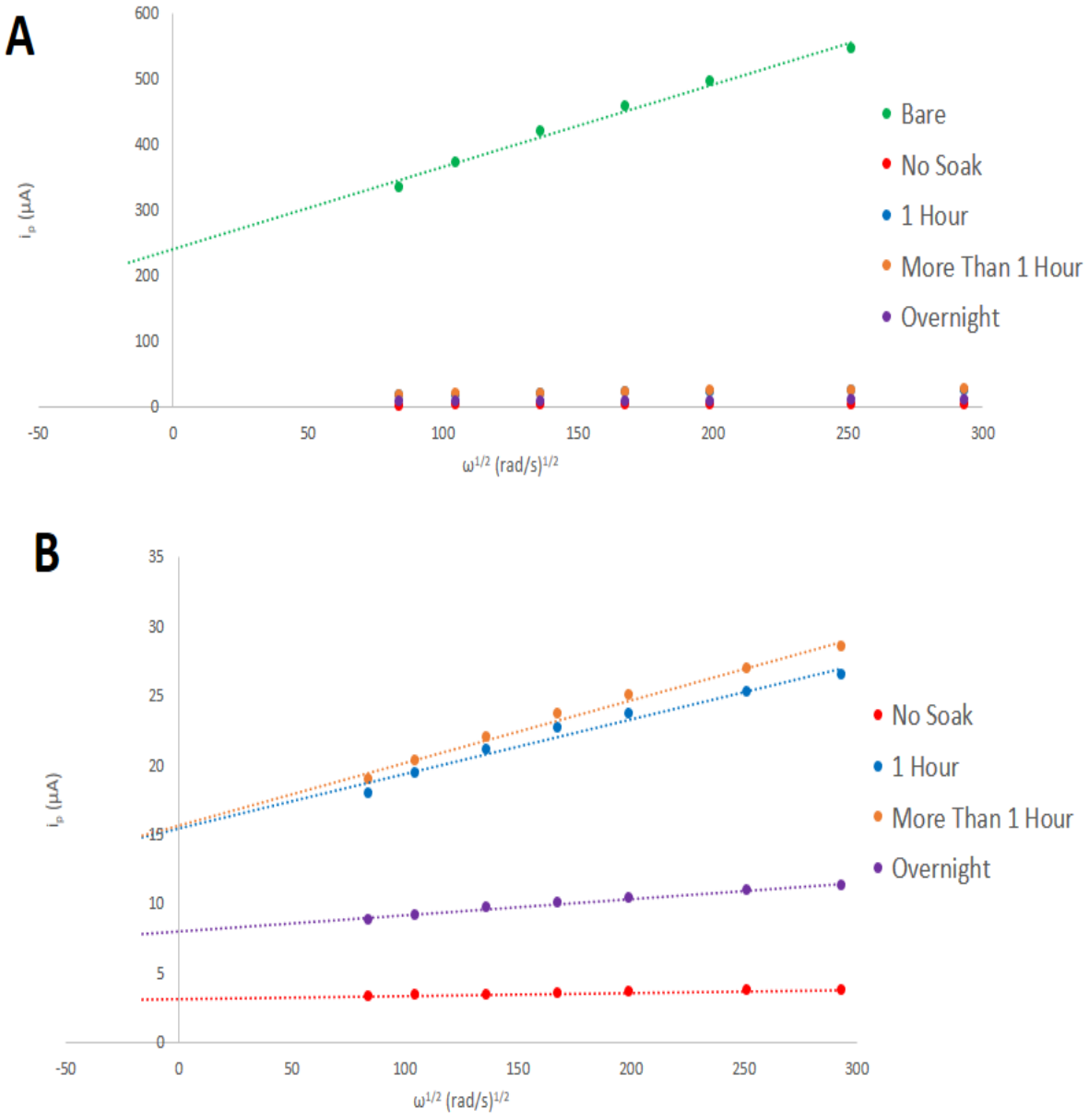

Figure 29. Levich plots of differing hydration times of Nafion membranes can be used with the Tedford Equation to determine a DE for each membrane. A) shows how bare greatly differs from the Nafion covered membranes with are seen on an expanded scale in B) where the bare data is excluded.

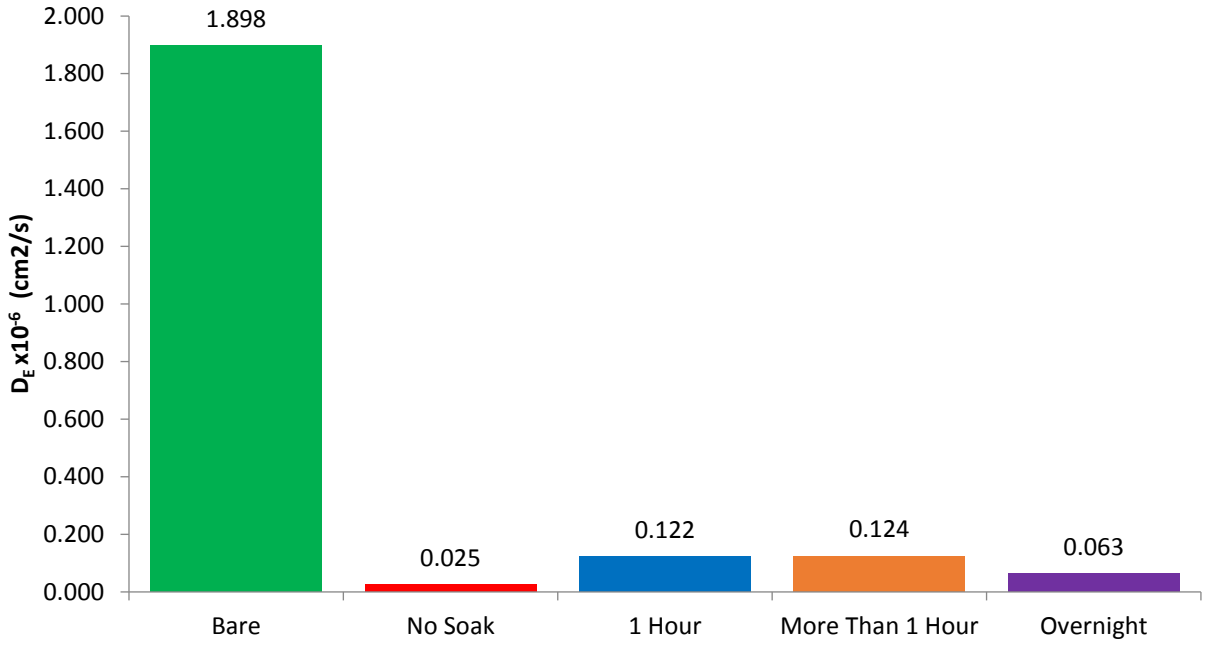

Figure 30. D_E is affected by the hydration time of the Nafion membrane.

The shorter hydration times have a larger D_E than non-hydrated membrane before decreasing again with the overnight soak. The decrease in D_E at longer soak times could be due to the electroosmotic drag (water molecules being "dragged" into or through the membrane with analyte molecules). During soaking, the ferricyanide slowly diffuses into the membrane along with additional nonconducting water molecules due to a concentration gradient driving force. Zawodzinski[46] observed this phenomenon with protons through Nafion 117 membranes. They determined the electroosmotic drag to be between 2.5 to 2.9 water molecules per proton for a fully hydrated membrane. They also observed that a partially hydrated membrane had an electroosmotic drag of 0.9 water molecules per proton. Breslau and Miller[47] had previously determined that the rate of the electroosmotic drag was dependent upon the charge density of the diffusing molecule and the size of the pore which can vary within the same membrane. For anions, the larger and more negatively charged molecules had a greater electroosmotic drag coefficient. In the present situation, the ferricyanide molecules could be dragging in pure,

nonconducting water through the membrane during the longer hydration periods causing an increase in the separation between redox centers (φ) and therefore a decrease in D_E (Eq. 5.1).

Other possibilities as to why there is a smaller D_E in the overnight soaked membranes is that the membrane is physically swelling outward (away from the electrode surface) therefore simply creating a longer pathway (δ_m) for the "electrons" to diffuse between the electrode surface and the bulk solution. Additionally, if ferricyanide stops incorporating into the membrane but water continues to hydrate and swell the membrane, then the distance between the redox centers within the membrane will increase as the membrane thickness increases.

Once the individual D_E has been determined for each membrane using the Tedford equation then this can further be used to investigate the redox centers within the membrane. The determined D_E can then be used in the Dahms-Ruff equation (Eq. 5.1) to determine the average distance between the redox centers within the membrane. If we assume the current signal is only due to the apparent diffusion of the electrons then the diffusion in the bulk (D) can be assumed to be zero. The k is the self-exchange rate constant for the ferri/ferrocyanide redox reaction and is $5x10^5$ M^{-1} s^{-1} according to Takagi and Swaddle.[48] The concentration of the analyte in the membrane (C_m) was determined in earlier (Section 3.4) to be 4mM. With these known variables input into the Dahms-Ruff equation, the determined average distances between the redox centers can be seen in Table 2. This is assuming that the redox centers are uniformly distributed throughout the membrane entire volume of the membrane between the electrode surface and the bulk solution. Under these assumptions, this would put about 40 molecules in line for the electron to use to get to the analyte in the bulk solution. These distances are larger than what Shiroishi et al.[49] observed using a ruthenium bipyridine derivative having average distances of 2.04nm within a Nafion membrane. Shiroishi was working with cations where ferricyanide is an

anion and it therefore makes sense that the ferricyanide distances are longer as the anion should not be in the negatively charged membrane to being with.

Soak Time	D_E	φ (µm)
No Soak	2.50E-08	0.126
1 Hour	1.22E-07	0.279
More Than 1 Hour	1.24E-07	0.281
Overnight	6.30E-08	0.200

Table 2. Using D_E to determine the average distance between redox centers in the Nafion membrane with the Dahms-Ruff equation.

5.6 Slopes of the Lines Using the Tedford Equation

The Levich treatment was developed for diffusion limited current at a bare electrode. The Levich treatment also applies to membrane covered electrodes, provided the membrane allows diffusion of the analyte through the membrane, or a conducting polymer, that allows for fast "apparent electron diffusion" through the membrane. In all of these cases the slope of the Levich line is a constant because it is based on bulk diffusion to the electrode. In the case here the apparent diffusion of electrons through the membrane is slow, and dominates the current response, to an applied potential. The Tedford Equation predicts a variable slope that depends on the concentration of the redox species in the film, Cm. The slopes in figure 29B decrease with soak time, compare hour soaks to overnight. The longer soaks contain more ferricyanide or Cm but the bulk concentration is the same. Therefore (C*− Cm) would be smaller for longer soaks and this is the case here, and supported by the more gradual slopes in Figure 29B. There is no data available to discuss the effects of apparent electrode area changes with soak time.

6 CONCLUSIONS

Nafion's use as a proton exchange membrane in a fuel cell can be improved by studying its degradation. One way to do this is by utilizing a probe molecule. Ferricyanide works well as a probe molecule because it is a large, negatively charge molecule that has already been extensively studied on a bare electrode. An intact Nafion membrane will block the ferricyanide from the electrode surface and no signal will be obtained. However, if there is a hole, tear, or other inconsistency in the membrane where the ferricyanide can reach the electrode surface then a signal will be obtained. In this way, ferricyanide as a probe molecule can be used as a diagnostic tool for Nafion membrane integrity in the time scale is short.

The Nafion membrane must be hydrated to conduct ions. To use ferricyanide as a diagnostic tool the membrane cannot have a previous prolonged exposure to ferricyanide as it can absorb into the membrane, albeit very slowly. The ferricyanide acts as redox centers in the membrane. The mechanism is not known precisely but can be one or some combination of electron hopping, charge transfer resistance, permeation, or diffusion with very slow kinetics. The Tedford Equation (Eq. 5.6) can be used to determine the apparent diffusion coefficient.

Both the probe molecule technique and the Tedford Equation could be used as diagnostic tools for fuel cell improvement. Using ferricyanide as a probe molecule could help in determining is a tear, hole, or fracture is present in the Nafion membrane used in the fuel cell. This could be done by mounting the membrane on an electrode surface capable of hydrodynamic voltammetry. This is a plausible technique as long as the membrane does not endure prolonged exposure to ferricyanide solution before the hydrodynamic voltammetry experiments are performed. Once the membrane is found to be free of any hole, tears, or fractures, the membrane can be soaked in a ferricyanide solution and the Tedford Equation employed to study the soaking

properties of the membrane. This can be expanded to other analytes that might be present in the fuel cell stack (such as catalyst compositions) that might poison or damage the PEM.

7 REFERENCES

1. Cheng, X.; Li, H.; Zheng, Q., *PEM Fuel Cell Diagn. Tools* **2012**, 491-513.

2. Curtin, D. E.; Lousenberg, R. D.; Henry, T. J.; Tangeman, P. C.; Tisack, M. E., *J. Power Sources* **2004,** *131* (1-2), 41-48.

3. Page, K. A.; Rowe, B. W., *ACS Symp. Ser.* **2012,** *1096* (Polymers for Energy Storage and Delivery: Polyelectrolytes for Batteries and Fuel Cells), 147-164.

4. Li, J. Y.; Nemat-Nasser, S., *Mechanics of Materials* **2000,** *32*, 303-314.

5. Bard, A. J.; Faulkner, L. R., Kinetics of Electrode Reactions. In *Electrochemical Methods: Fundamentals and Applications*, John Wiley & Sons, Inc.: Hoboken, NJ, 2001; Vol. 2, pp 87-136.

6. Laviron, E., *Journal of Electroanalytical Chemistry* **1979,** *100*, 263-270.

7. LaConti, A. B.; Fragala, A. R.; Boyack, J. R., *Proc. - Electrochem. Soc.* **1977,** *77-6* (Proc. Symp. Electrode Mater. Processes Energy Convers. Storage), 354-74.

8. Congress, U. S. L. o. Who Invented the Automobile? (accessed February 19).

9. Transportation, U. S. D. o. Table 1-11: Number of U.S. Aircraft, Vehicles, Vessels, and Other Conveyances. (accessed February 19).

10. History, N. M. o. A. **Transportation Technology Videos**Transportation Technology Videos. (accessed February 19).

11. Schoenbein, C. F., *Philosophical Magazine Series 3* **1839,** *14* (85), 43-45.

12. Grove, W. R., *Philosophical Magazine Series 3* **1839,** *14* (86), 127-130.

13. Bossel, U., *The Birth of the Fuel Cell, 185-1845*. European Fuel Cell Forum: Oberrohrdorf, Switzerland, 2000.

14. Flintoff, C. Where Does America Get Oil? You May Be Surprised. (accessed October 24, 2016).

15. Oxtoby, D. W.; Gillis, H. P.; Campion, A., Spontaneous Processes and Thermodynamic Equlibrium. In *Principles of Modern Chemistry*, 7 ed.; Brooks/Cole, Cengage Learning: Belmont, CA, 2012; p 574.

16. Vanýsek, P., Electrochemical Series. In *CRC Handbook of Chemistry and Physics*, 92 ed.; Haynes, W. M., Ed. CRC Press: Boca Raton, FL, 2011; pp 5-80 - 5-89.

17. Bakker, E.; Pretsch, E., Advances in Potentiometry. In *Electroanalytical Chemistry*, Bard, A. J.; Zoski, C., Eds. CRC Press Taylor & Francis Group: Boca Raton, FL, 2012; Vol. 24, pp 1-73.

18. Unnikrishnan, E. K.; Kumar, S. D.; Maiti, B., *Journal of Membrane Science* **1997,** *137*, 133-137.

19. Konopka, S. J.; McDuffie, B., *Analytical Chemistry* **1970,** *42* (14), 1741-1746.

20. Roffel, B.; Van de Graaf, J. J., *Journal of Chemical and Engineering Data* **1977,** *22* (3), 300-302.

21. Legrand, J.; Dumont, E.; Comiti, J.; Fayolle, F., *Electrochimica Acta* **2000,** *45* (11), 1791-1803.

22. Ghostine, R. A.; Schlenoff, J. B., *Langmuir* **2011,** *27*, 8241-8247.

23. Y.S., G.; M.J., S.; S.A., G.; K.M., W.; G.A., C.; M., T., *Chemical Communications* **2013,** *49* (15), 1551-1553.

24. Moldenhauer, J.; Meier, M.; Paul, D. W., *Journal of the Electrochemistry Society* **2016,** *163* (8), H672-H678.

25. Tobias, C. W.; Eisenburg, M.; Wilke, C. R., *Journal of the Electrochemical Society* **1952,** *99* (12), 359C-365C.

26. Liu, W.; Ruth, K.; Rusch, G., *Journal of New Materials for Materials for Electrochemical Systems* **2001,** *4*, 227-231.

27. Bard, A. J.; Faulkner, L. R., Methods Involving Forced Convection - Hydrodynamic Methods. In *Electrochemical Methods: Fundamentals and Applications*, John Wiley & Sons, Inc.: Hoboken, NJ, 2001; Vol. 2, pp 331-367.

28. Eisenburg, M.; Tobias, C. W.; Wilke, C. R., *Journal of the Electrochemical Society* **1954,** *101* (6), 306-320.

29. Adigoppula, V. K. A Study on Nafion Nanocomposite Membranes for Proton Exchange Membrane Fuel Cells. Wichita State University, Wichita, KS, 2011.

30. Ehrlich, P., *Journal of Research of the National Bureau of Standards* **1953,** *51* (4), 185-188.

31. Mauritz, K. A.; Moore, R. B., *Chemical Reviews* **2004** *104* (10), 4535-4585.

32. BUPERS, Capacitance. In *Fundamentals of Electronics, Basic Electricity, Alternating Current NAVPERS 93400A-1b*, Bureau of Navy Personnel, United States Navy: Arlington, VA, 1965; Vol. 1B, p 201.

33. Neff, V. D., *Journal of the Electrochemical Society* **1978,** *125* (6), 886-887.

34. Bordwell, F. G.; Algrim, D., *Journal of Organic Chemistry* **1976,** *41* (14), 2507-2508.

35. Eaton, W. A.; George, P.; Hanania, G. I. H., *Journal of Physical Chemisty* **1967,** *71* (7), 2016-2021.

36. Korzeniewski, C.; Severson, M. W.; Schmidt, P. P.; Pons, S.; Fleischmanna, M., *Journal of Physical Chemistry* **1987,** *91*, 5568-5573.

37. Kuta, J.; Yeager, E., *Journal of Electroanalytical Chemistry and Interfacial Electrochemistry* **1975,** *59*, 110-112.

38. Frumkin, A. N.; Damaskin, B. B., *Modern Aspects of Electrochemistry* **1964,** *3*, 149-223.

39. Smith, C. P.; White, H. S., *Analytical Chemistry* **1992,** *64* (2), 2398-2405.

40. Bard, A. J.; Faulkner, L. R., Electroactive Layers and Modified Electrodes. In *Electrochemical Methods: Fundamentals and Applications*, John Wiley & Sons, Inc.: Hoboken, NJ, 2001; Vol. 2, pp 580-631.

41. Gough, D. A.; Leypoldt, J. K., *Analytical Chemistry* **1979,** *51* (3), 439-444.

42. Marcus, R. A., *Reviews of Modern Physics* **1993,** *65* (3), 599-610.

43. White, H. S.; Leddy, J.; Bard, A. J., *Journal of the American Chemical Society* **1982,** *104* (18), 4811-4817.

44. Majda, M., Translational Diffusion and Electron Hopping in Monolayers at the Air/Water Interface. In *Thin Films: Organic Thin Films and Surfaces. Directions for the Nineties*, Ulman, A., Ed. Academic Press: Cambridge, MA 1995; Vol. 20, pp 331-347.

45. DeWulf, D.; Bard, A. J., *J. Macromol. Sci., Chem.* **1989,** *A26* (8), 1205-9.

46. Zawodzinski, T. A.; Derouin, C.; Radzinski, S.; Sherman, R. J.; Smith, V. T.; Springer, T. E.; Gottesfeld, S., *J. Electrochem. Soc.* **1993,** *140* (4), 1041-1047.

47. Breslau, B. R.; Miller, I. F., *Industrial & Engineering Chemistry Fundamentals* **1971,** *10* (4), 554-565.

48. Takagi, H.; Swaddle, T. W., *Inorganic Chemistry* **1992,** *31*, 4669-4673.

49. Shiroishi, H.; Ishikawa, K.; Hirano, K.; Kaneko, M., *Polymers for Advanced Technologies* **2001,** *12* (3-4), 237-243.